

**MODELLING OF HIGH EFFICIENCY MINIATURE AEROCYCLONE**

**AIMAN HAKIM BIN BADARISMAN**

**UNIVERSITI MALAYSIA PAHANG**

UNIVERSITI MALAYSIA PAHANG

**BORANG PENGESAHAN STATUS TESIS**

JUDUL: MODELLING OF HIGH EFFICIENCY MINIATURE AEROCYCLONE

SESI PENGAJIAN: 2009/2010

Saya **AIMAN HAKIM BIN BADARISMAN**

mengaku membenarkan kertas projek ini disimpan di Perpustakaan Universiti Malaysia Pahang dengan syarat-syarat kegunaan seperti berikut :

1. Hakmilik kertas projek adalah di bawah nama penulis melainkan penulisan sebagai projek bersama dan dibiayai oleh UMP, hakmiliknya adalah kepunyaan UMP.
2. Naskah salinan di dalam bentuk kertas atau mikro hanya boleh dibuat dengan kebenaran bertulis daripada penulis.
3. Perpustakaan Universiti Malaysia Pahang dibenarkan membuat salinan untuk tujuan pengajian mereka.
4. Kertas projek hanya boleh diterbitkan dengan kebenaran penulis. Bayaran royalti adalah mengikut kadar yang dipersetujui kelak.
5. \*Saya membenarkan/tidak membenarkan Perpustakaan membuat salinan kertas projek ini sebagai bahan pertukaran di antara institusi pengajian tinggi.
6. \*\* Sila tandakan (✓ )

SULIT

(Mengandungi maklumat yang berdarjah keselamatan atau kepentingan Malaysia seperti yang termaktub di dalam AKTA RAHSIA RASMI 1972)

TERHAD

(Mengandungi maklumat TERHAD yang telah ditentukan oleh organisasi/badan di mana penyelidikan dijalankan).

TIDAK TERHAD

Disahkan oleh

(TANDATANGAN PENULIS)

Alamat Tetap: **91, FASA 1B, TMN BKT KEPAYANG,**

**70200 SEREMBAN, N. SEMBILAN.**

(TANDATANGAN PENYELIA)

**DR JOLIUS GIMBUN**

Tarikh:

Tarikh:

- CATATAN:
- \* Potong yang tidak berkenaan.
  - \*\* Jika Kertas Projek ini SULIT atau TERHAD, sila lampirkan surat daripada pihak berkuasa/organisasi berkenaan dengan menyatakan sekali tempoh tesis ini perlu dikelaskan sebagai SULIT atau TERHAD.
  - ♦ Tesis ini dimaksudkan sebagai tesis bagi Ijazah Doktor Falsafah dan Sarjana secara penyelidikan, atau disertasi bagi pengajian secara kerja kursus dan penyelidikan, atau Laporan Projek Sarjana Muda (PSM)

**MODELLING OF HIGH EFFICIENCY MINIATURE AEROCYCLONE**

**AIMAN HAKIM BIN BADARISMAN**

A thesis submitted in fulfillment of the  
requirements for the award of the degree of  
Bachelor of Chemical Engineering

**Faculty of Chemical and Natural Resources Engineering  
Universiti Malaysia Pahang**

APRIL 2010

“I hereby declare that I have read this thesis and in my opinion this thesis has fulfilled the qualities and requirements for the award of Degree of Bachelor of Engineering (Chemical)”

Signature : .....

Supervisor : DR JOLIUS GIMBUN

Date :

## DECLARATION

I declare that this thesis entitled “*Modelling of High Efficiency Miniature Aerocyclone*” is the result of my own research except as cited in the references. The thesis has not been accepted for any degree and is not concurrently submitted in candidature of any other degree.

Signature : .....

Name : AIMAN HAKIM BIN BADARISMAN

Date :

**DEDICATION**

*To my beloved parent Abah, Mama, Atok, Uwan, and  
siblings,*

## ACKNOWLEDGEMENT

At first I want thanked to Ilahi for all those good blessings as I tend to finished this research with a great condition. This research, did gave me big impact in my life as I able to managed and hold the responsible to strive to the fullest effort. I do believe in phrase “Practice makes Perfect” as during the first trial of the simulation the result is quite handful and disappointing, as everything starts from zero. But when it comes to the second and third trials, everything is much easier and I tend to solve the problems smoothly. I want to thank to all people around who do care and help me out when it comes to difficulties. Thank you very much.

Besides that, I would like to give my deepest gratitude to my supervisor, Dr. Jolius Gimibun for his tireless effort and on-going support, for all the guidance and useful tips in handling the simulation works and also in finishing the report. Without his help, this thesis would not be this perfect. In addition, I want to thank Mr. Mohd Shahimie Selamat and Miss Siti Ferdaus for all of their effort to help me construct the simulation and teach me how to extract those important data from Fluent software.

Other than that, I feel so blessed with all the motivations from my fellow friends, roommates and also my lab partner, Mohd Shahimie Selamat, Siti Ferdaus Aspari and Masita Md Shah. I hope this friendship will never end. I love all of my friends, I do hopes that they will never forget all those memories we cherished together.

Not forgetting my lovely family who always giving me the fullest love, energy and moral support in completing my thesis. Even they do not contribute as much effort in this research, their strength do keep me motivated to do the best. I will never let my family down as they giving so much trust and in me. Thank you.

## ABSTRACT

Cyclone separation is one of the largely recognized methods of removing particulate in air, gas or water stream without help from filters. Cyclone is favourite separation device in various industries due to its simplicity, inexpensive design and minimum operational cost. In this research, the objective is maximizing the performance of miniature aerocyclone. The performance of aerocyclone can be analyzed by its collection efficiency and pressure drop. In past studies, expensive and time consuming experiment were conducted in order to analyze the performance of cyclone, but Computational Fluid Dynamics (CFD) software that being implemented in this research has successfully solve the problem. FLUENT is a commercially available CFD code that utilizes the finite volume formulation to carry out coupled or segregated calculations. For the turbulent flow in a cyclone the key to the success of CFD lies with the accurate description of the turbulent behavior of the flow. The simulation methodologies involve 5 steps before the simulation data can be verified with experimental data. The simulation starts with meshing of miniature cyclone via Gambit software. The meshed cyclone was then transferred into FLUENT software for simulation, where all the boundary condition is programmed in the software. After simulation completed, the data was then extracted and converted in the function of cyclone collection efficiency and pressure drop. The results show the influence of inlet velocity and exit tube size on cyclone performance and significant conclusion were made. The performances of turbulence model used in the simulation were then compared.



## ABSTRAK

Pemisahan menggunakan alat siklon adalah salah satu kaedah yang diakui sebahagian besar sangat berkesan mengasing partikel di udara, gas, atau air sungai tanpa bantuan daripada penapis. Siklon adalah peranti pemisahan lazim di pelbagai industri kerana kesederhanaan rekaan dan kos operasi yang minimum. Objektif utama kajian ini adalah memaksimumkan prestasi mini siklon udara menggunakan teknologi Computational Fluid Dynamics (CFD). Prestasi asiklon udara boleh dianalisis dari kecekapan pungutan partikel dan perbezaan tekanan didalam siklon. Daripada kajian silam, kaedah eksperimen ternyata mahal dan memakan masa dalam menganalisis prestasi siklon. Perisian Computational Fluids Dynamics (CFD) yang diimplementasikan di dalam kajian ini telah berjaya mengatasi masalah tersebut. FLUENT adalah kod CFD sedia ada komersil yang memanfaatkan formulasi tentu isipadu dalam melaksanakan pengiraan secara pasangan dan mahupun terpisah. Kunci utama ketepatan analisa CFD terhadap aliran turbulen bergantung pada input data yang tepat untuk perilaku turbulen. Metodologi simulasi melibatkan 5 langkah sebelum data simulasi boleh disahkan dengan data eksperimen. Simulasi bermula dengan kaedah “meshing” model maya mini siklon menggunakan perisian Gambit. Siklon yang telah di’mesh’ kemudian dipindahkan ke dalam software FLUENT untuk simulasi, di mana semua keadaan had diprogramkan dalam perisian FLUENT. Setelah selesai simulasi, data kemudian diekstrak dan diterjemah dalam fungsi kecekapan pengumpulan dan perbezaan tekanan didalam siklon. Prediksi CFD menunjukkan kelajuan masuk udara dan dimensi tiub keluar siklon amat mempengaruhi prestasi siklon, sesuai dengan data eksperimen. Model turbulen (RSM & DES) yang digunakan dalam simulasi kemudian dibandingkan prestasinya.

## TABLE OF CONTENT

| CHAPTER  | TITLE   | PAGE |
|----------|---|------|
|          | TITLE PAGE  | i    |
|          | SUPERVISOR DECLARATION                              | ii   |
|          | DECLARATION   | iii  |
|          | DEDICATION  | iv   |
|          | ACKNOWLEDGEMENT                                     | v    |
|          | ABSTRACT  | vi   |
|          | ABSTRAK   | vii  |
|          | TABLE OF CONTENT                                    | viii |
|          | LIST OF TABLE                                       | xi   |
|          | LIST OF FIGURES                                     | xii  |
|          | LIST OF SYMBOLS                                     | xiv  |
| <b>1</b> | <b>INTRODUCTION</b>                                 |      |
|          | 1.0 Introduction                                    | 1    |
|          | 1.1 Computational Fluid Dynamics (CFD)              | 3    |
|          | 1.2 Research Objectives                             | 5    |
|          | 1.3 Problem Statement                               | 5    |
| <b>2</b> | <b>LITERATURE REVIEW</b>                            |      |
|          | 2.0 Introduction                                    | 7    |
|          | 2.1 Studies on Cyclone Performance                  |      |
|          | 2.1.1 Effect of Vortex Finder and Cone Dimension on |      |

|          |  |    |
|----------|--|----|
|          | Cyclone Performance  | 9  |
|          | 2.1.2 Effect of Inlet Velocity on Cyclone Performance                      | 9  |
|          | 2.1.3 Effect of Temperature on Cyclone Performance                         | 11 |
|          | 2.1.4 50% Particle Cut-Off Diameter  | 12 |
|          | 2.1.5 Review on Experimental and Simulation Studies on Cyclone Performance | 13 |
|          | 2.2 Uses of Cyclone Separation   |    |
|          | 2.2.1 Cyclone Gasifier in Biomass Plant                                    | 18 |
|          | 2.2.2 Hydro-Cyclone Separation   | 19 |
|          | 2.2.3 Circulating Fluidized Bed (CFB) Reactor                              | 20 |
| <b>3</b> | <b>METHODOLOGY</b>   |    |
|          | 3.0 Introduction   | 21 |
|          | 3.1 CFD Modelling Approach   |    |
|          | 3.1.1 Simulation Procedure   | 22 |
|          | 3.1.1.1 Identification of Physical Problem                                 | 23 |
|          | 3.1.1.2 Pre-processing/meshing   | 23 |
|          | 3.1.1.3 Numerical Model Setup  | 25 |
|          | 3.1.1.4 Solution Computation & Monitoring                                  | 25 |
|          | 3.1.1.5 Post-processing in Fluent  | 26 |
|          | 3.1.1.6 Verification of CFD model  | 26 |
|          | 3.1.2 Cyclones Design  | 27 |

|          |  |    |
|----------|--|----|
|          | 3.2 Numerical Modeling of the Cyclone                    | 28 |
|          | 3.2.1 Governing Equation for Fluid Flow inside a Cyclone | 29 |
|          | 3.2.2 Turbulence Model                                   | 30 |
|          | 3.3 Details on CFD Setting                               | 35 |
| <b>4</b> | <b>RESULT AND DISCUSSION</b>                             |    |
|          | 4.0 Introduction   | 36 |
|          | 4.1 Cyclone Collection Efficiency                        | 36 |
|          | 4.2 Cyclone Pressure Drop                                | 43 |
|          | 4.3 Particle 50% Cut-Off Size                            | 44 |
| <b>5</b> | <b>CONCLUSION</b>  |    |
|          | 5.0 Conclusions  | 47 |
|          | 5.1 Future Works   | 48 |
|          | <b>REFERENCES</b>  |    |
|          | <b>APPENDIX</b>  |    |

**LIST OF TABLES**

| <b>TABLE</b> | <b>TITLE</b>   | <b>PAGE</b> |
|--------------|--|-------------|
| 2.1          | Review on Experimental and Simulation Researches     | 14          |
| 3.1          | Dimensions of Tested Cyclones                        | 27          |
| 3.2          | Details on CFD Setting                               | 35          |
| 4.1          | Fluent predictions for cyclone I & II pressure drop  | 44          |
| 4.2          | Fluent predictions for cyclone 50% cut-off diameter. | 46          |

## LIST OF FIGURES

| FIGURE NO. | TITLE   | PAGE |
|------------|---|------|
| 1.1        | Miniature Aero-cyclone  | 2    |
| 1.2        | The applications of CFD in simulating dynamics behavior of F1 car, airplane and cyclone separation.   | 5    |
| 2.1        | Vortex finder of a cyclone  | 9    |
| 3.1        | Steps for CFD Modelling   | 22   |
| 3.2        | Coarse grid cyclone mesh  | 24   |
| 3.3        | Cyclone Dimension   | 28   |
| 4.1        | Simulated collection efficiencies for Kim & Lee cyclone I ( $P = 1 \text{ atm}$ , $T = 273 \text{ K}$ , $v_i = 8.8 \text{ lpm}$ , $D_e = 0.8 \text{ cm}$ )  | 37   |
| 4.2        | Simulated collection efficiencies for Kim & Lee cyclone I ( $P = 1 \text{ atm}$ , $T = 273 \text{ K}$ , $v_i = 12.4 \text{ lpm}$ , $D_e = 0.8 \text{ cm}$ ) | 37   |
| 4.3        | Simulated collection efficiencies for Kim & Lee cyclone I ( $P = 1 \text{ atm}$ , $T = 273 \text{ K}$ , $v_i = 18.4 \text{ lpm}$ , $D_e = 0.8 \text{ cm}$ ) | 38   |

|     |   |    |
|-----|---|----|
| 4.4 | Simulated collection efficiencies for Kim & Lee cyclone II ( $P = 1$ atm, $T = 273$ K, $v_i = 8.8$ lpm, $D_e = 1.36$ cm)  | 38 |
| 4.5 | Simulated collection efficiencies for Kim & Lee cyclone II ( $P = 1$ atm, $T = 273$ K, $v_i = 12.4$ lpm, $D_e = 1.36$ cm) | 39 |
| 4.6 | Simulated collection efficiencies for Kim & Lee cyclone II ( $P = 1$ atm, $T = 273$ K, $v_i = 18.4$ lpm, $D_e = 1.36$ cm) | 39 |
| 4.7 | RSM prediction of collection efficiency for two different tube sizes, cyclone 1 & 2 for $v_i = 18.4$ lpm                  | 41 |
| 4.8 | Pressure profile of cyclone as simulated by FLUENT.   | 44 |

**LIST OF SYMBOLS**

|           |   |                                    |
|-----------|---|------------------------------------|
| L         | - | Natural length (m)                 |
| a         | - | cyclone inlet height (m)           |
| b         | - | cyclone inlet width (m)            |
| D         | - | cyclone body diameter (m)          |
| <i>De</i> | - | cyclone gas outlet diameter (m)    |
| H         | - | cyclone height (m)                 |
| <i>h</i>  | - | cyclone cylinder height (m)        |
| $\mu$     | - | Viscosity of liquid (Pa.s)         |
| h         | - | Heat transfer coefficient          |
| °C        | - | Degree Celsius                     |
| kg        | - | Kilogram                           |
| K         | - | Degree Kelvin                      |
| m         | - | Meter                              |
| S         | - | cyclone gas outlet duct length (m) |
| B         | - | cyclone dust outlet diameter (m)   |
| $d_p$     | - | particle diameter (m)              |
| $v_i$     | - | inlet velocity (m/s)               |
| $C_D$     | - | Drag Coefficients                  |



## CHAPTER 1

### INTRODUCTION

#### 1.0 Introduction

Cyclone separation is one of the largely recognized methods of removing particulate in air, gas or water stream without help from filter. These particulates are removed through spinning, often turbulent, flow of fluid plus a little help from gravity. The device is called a cyclone. A conventional cyclone looks like a cylindrical or conical where high velocity air rotating within it. At the top of the cyclone (wide end) air flow as vortex and end up at the narrow end or the bottom of the cyclone. The air flow then goes out through top in a straight stream via center of the cyclone, meanwhile denser particle in the rotating stream have too much inertia to follow the tight curve of the stream and strike the outside wall, falling then to the bottom of the cyclone where they can be removed. Within the conical section of the cyclone the rotational radius of stream is reduced whenever the flow move nearer to the narrow bottom end, thus separating smaller and smaller particles. The outlet flow at the top end often labeled as major flow meanwhile the outlet flow at bottom where dust container is placed often labeled as minor flow. A cyclone where the minor flow is pumped out from its container is called virtual cyclones.

Compared to other gas–solid separation methods, such as filters, scrubbers, and settlers, cyclone separators are simpler to construct, easier to maintain, require lower capital and operating costs, are more compact, and versatile. Especially at high

temperatures and pressures, the cyclone is often the only viable economical separation process (Wang et al., 2010). Cyclones low capital cost and seldom maintenance operation make them suitable for use as pre-cleaners for more expensive final control devices such as bag-houses or electrostatic precipitators. Cyclone can also be beneficial to human health. For examples, in a saw-mill or a power plant, large scale cyclone is use to removed sawdust or coal dust from the air. Both sawdust and coal dust are dangerous when enters human respiratory system. In oil refinery industries, large scale cyclone is used to separate oil and gases meanwhile in cement industries; cyclone is implemented as one of the component of kiln pre-heaters.

Large cyclones are used to remove particles from industrial gas streams, while small cyclones (see figure 1.1) are used to separate particles for ambient sampling (Kim et al., 2001). With mini cyclone, fine particle as small as dust can be separated from air. Due to its size, mini cyclones can be located in various places, making it suitable for analysis instruments. Small cyclones are in the use of the so-called personal cyclones for the selective sampling of various air-laden respirable particles in occupational hygiene and environment control. The cyclones which are used in these special circumstances are usually very small in size with the typical working flow rate of a personal cyclone being about 2 liter/min in order to sample particles of just a few microns in diameter. Personal cyclones used in occupational hygiene and environment hygiene often use light battery-operated pumps which are available with a flow rate up to 4-5 liter/min.



Figure 1.1: Miniature Aero-cyclone

When engineers want to design a cyclone, there are two important parameters that need to be considered. These parameters are collection efficiency of particle and pressure drop across the cyclone. An accurate prediction of cyclone pressure drop is very important because it relates directly to operating costs. Higher inlet velocities give higher collection efficiencies for a given cyclone, but this also increases the pressure drop across the cyclone (Gimbun et al. 2004). Particle size distribution is also strongly influence the collection efficiency. Cyclone collection efficiencies can reach 99% for particles bigger than 5  $\mu\text{m}$  (Silva et al. 2003). Their simple design, low maintenance costs, and adaptability to a wide range of operating conditions such as sizes and flow rates make cyclones one of the most widely used particle removal devices. By using suitable materials and methods of construction, cyclones may be adapted for use in extreme operating conditions: high temperature, high pressure, and corrosive gases (Gimbun et al. 2004).

### **1.1 Computational Fluid Dynamics (CFD)**

Miniature cyclone will be modeled using Computational Fluid Dynamics (CFD). CFD is a computational technology that enables study of the dynamics of things that flow. Using CFD, one can build a computational model that represents a system or device that is want to studied. The fluid flow physics and chemistry is applied to this virtual prototype, and the software will output a prediction of the fluid dynamics and related physical phenomena. Therefore, CFD is a sophisticated computationally-based design and analysis technique. CFD software gives the capabilities to simulate flows of gases and liquids, heat and mass transfer, moving bodies, multiphase physics, chemical reaction, fluid-structure interaction and acoustics through computer modeling. Using CFD software, one can build a 'virtual prototype' of the system or device that one wish to analyze and then apply real-world physics and chemistry to the model, and the software will provide images and data, which predict the performance of that design.

The CFD solver does the flow calculations and produces the results. Four general-purpose products: FLUENT, FloWizard, FIDAP, and POLYFLOW. FLUENT is used in most industries. FloWizard is the first general-purpose rapid flow modeling tool for design and process engineers built by Fluent. POLYFLOW (and FIDAP) are also used in a wide range of fields, with emphasis on the materials processing industries.

The FLUENT CFD code has extensive interactivity; changes can be made to the analysis at any time during the process. These saves time and enable design refines more efficiently. The graphical user interface (GUI) is intuitive, which helps to shorten the learning curve and make the modeling process faster. It is also easy to customize physics and interface functions to specific needs. In addition, FLUENT's adaptive and dynamic mesh capability is unique among CFD vendors and works with a wide range of physical models. This capability makes it possible and simple to model complex moving objects in relation to flow.

FLUENT as a commercially available CFD code utilizes the finite volume formulation to carry out coupled or segregated calculations (with reference to the conservation of mass, momentum and energy equations). It is suitable for incompressible to mildly compressible flows. The conservation of mass, momentum and energy in a fluid flow are expressed in terms of non-linear partial differential equations that generally defy solution by analytical means. The solution of these equations has been made possible by the advent of powerful workstations, as available in Universiti Malaysia Pahang (UMP) Process Control Lab, opening avenues towards the calculation of complicated flow fields with relative ease. Figure 1.2 shows the analysis of dynamic behaviour of various objects using CFD software.

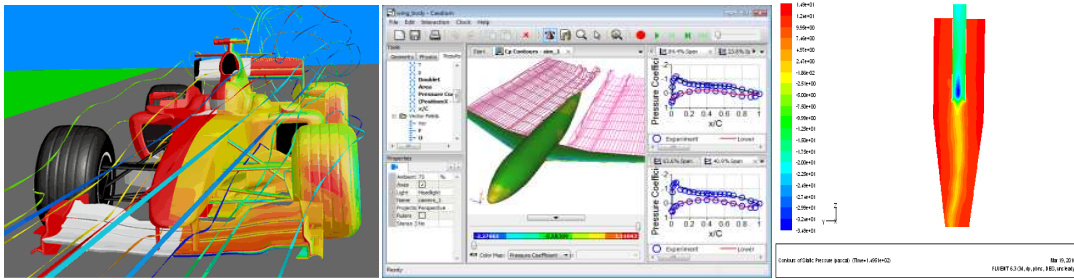


Figure 1.2: The applications of CFD in simulating dynamics behavior of F1 car, airplane and cyclone separation.

## 1.2 Research Objectives

The following are the objectives of this research:

- 1) To evaluate the influence of vortex finder dimension and inlet velocity on miniature aero-cyclone collection efficiency and pressure drop
- 2) Modeling high efficiency miniature aero-cyclone using Computational Fluids Dynamic (CFD)

## 1.3 Problem Statement

The pressure drops and collection efficiency are evidently the most important features from the point of view of cyclonic operation. At the end of this research we want to see the relationship of these two features with the design and operating parameters, or the manipulated parameters. Manipulated parameters for this research are vortex finder dimension and inlet velocity. In the past, the only way to determine the collection efficiency and pressure drop of cyclone operation is via experiment. Let say we want to distinguish the effect of two cyclones with different tip diameters towards pressure drop; experimentally we have to build the prototypes of these two different cyclones. These prototypes then operated and pressure across the cyclone is measured. Finally the data is

compared between the two cyclones before conclusions were drawn. These works require plenty of time and investment moreover if we have many design parameters to be tested. Online Master-sizer and LDA are the instruments used to determine the cyclone collection efficiency and pressure drop experimentally, and they are not come cheap. This is where simulation technology comes in handy. Over the year, computer and software technology has advances so much where the effect of design parameter on cyclone can now be simulated with one simple click. Thus, CFD is fully utilized in this study to understand the behavior of cyclone separation.

## CHAPTER 2

### LITERATURE REVIEW

#### 2.0 Introduction

With growing concern for the environmental effects of particulate pollution, it is becoming increasingly important to be able to optimize the design of pollution control systems; the separation of solid particles is also required in many industrial processes. For this purpose, cyclone separators are widely used as the most common devices. Conventionally, cyclone separators have been used as pre-cleaning devices for the removal of particles bigger than 10  $\mu\text{m}$  from the carrier gas in both air pollution control and other processes. Because of their adaptability, simple design and low costs in terms of maintenance, construction and operation, those properties make cyclones ideal for use in the various stages of industrial applications.

Due to cyclone effectiveness in industry, numerous researches were conducted related to influence of cone tip diameter, particle size distribution, vortex finder dimension, inlet velocity, cyclone height and operating temperature on miniature aero-cyclone collection efficiency and pressure drop. In the last few decades, the majority of the research on cyclones has focused on large industrial cyclones and a number of predictive models have been developed which attempt to predict key performance parameters, such as the characteristics of the separation efficiency and the pressure drop across the cyclone. The need to improve the collection efficiency of a cyclone has existed

since the early 1950, where Linden (1949), Lapple (1950), and Stairmand (1952) did their research on particulate removal from contaminated gas streams in industrial processes. Pressure drops across the cyclone plays a great deal in determining the performance of cyclone, where usually researchers conclude the pressure drop change along with collection efficiency, for example Kim & Lee (1990), Griffith & Boysan (1996), Kim et al. (2001), and Chuah et al. (2006).

Miniature cyclone was comprehensively studied when industrial hygiene awareness significantly increases in the public eye. In the case of health-related personal cyclones, more strict standards are enforced on industrial hygiene than is the situation for cyclones which are used in industrial processes and this has been outlined by Kenny (1996). In order to model the behaviour of the human breathing, personal cyclones are required to possess a particle size-selection (or penetration/separation) curve which follows specific sampling convention, for example the ISO international sampling convention (Ma et al., 2000). In recent years, a great deal of effort has continuously been contributed to the research on small sampling cyclones, for example studies made by Chan and Lippmann, 1977; Liden and Kenny, 1991, 1992; Overcamp and Scarlett, 1993; Maynard and Kenny, 1995; Kenny and Gussman, 1997. It is found that most of the existing predictive models for cyclones are experimentally based semi-empirical models and do not have a profound fluid mechanics basis. Therefore, they are often limited in their use to some special type of cyclones. The design of new cyclones for specific applications often rely on performing numerous and very costly experimental investigations. It is not until recently that relatively rapid and accurate methods have become available to measure the particle size-selective characteristics of small personal cyclones.



## 2.1 Studies on Cyclone Performance

### 2.1.1 Effect of Vortex Finder and Cone Dimension on Cyclone Performance

Vortex finder can also be referred to the exit tube of the cyclone which is fixed on the top of the cyclone and it protrudes some distance into the body of the cyclone (refer figure). The vortex finder size is an especially important dimension, which significantly affect the cyclone performance as its size plays a critical role in designing the flow field inside the cyclone, including the pattern of the outer and inner spiral flows. Saltzman and Hochstrasser (1983) studied the design and performance of miniature cyclones for respirable aerosol sampling, each with a different combination of three cyclone cone lengths and three vortex finder diameters. Iozia and Leith (1989) optimized the cyclone design parameters, including the vortex finder diameter, to improve the cyclone performance using their optimization program. Lim et al. (2003) found that the collection efficiencies of the cyclones with the cone-shaped vortex finders varied slightly, thus they conclude that cone shapes or lengths of cone-shaped vortex finder are not an important factor in affecting the particle collection efficiencies. Meanwhile Kim & Lee (1990) believes that the exit tube size plays a critical role in defining the flow field inside the cyclone, including the pattern of the outer and inner spiral flows.

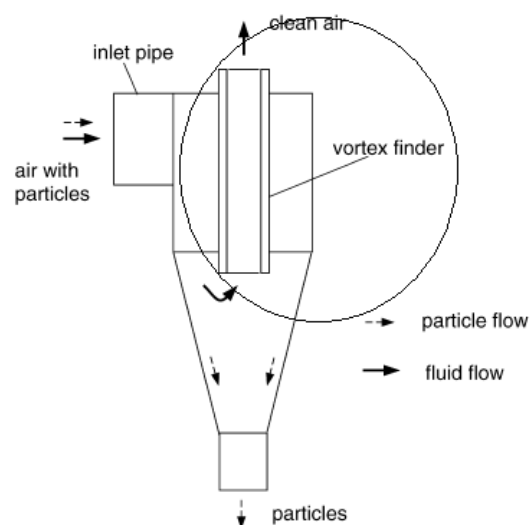


Figure 2.1: Vortex finder of a cyclone

The cone dimension of a cyclone is actually influential on cyclone performance even though it was usually neglected in many cyclone body dimension researches. The cone was considered only for practical purpose of delivering collected particles into bottom discharge point. Chuah et al. (2005) proves cyclone with a smaller cone diameter result slightly higher collection efficiency compared to the cyclone with a bigger cone diameter using CFD simulation. The simulation were done using two turbulence model, RNG k- $\epsilon$  and RSM based on Xiang et al. (2001) experiment.

### **2.1.2 Effect of Inlet Velocity on Cyclone Performance**

Inlet velocity of mixture between gas and particle was proven influential to cyclone performance. Inlet velocity can be obtained by dividing the volume flow rate of inlet with inlet area of the cyclone vane. Gimbut et al. (2004) stated that for the identical size and configuration of cyclone, the higher the gas inlet velocity is, the sharper the efficiency would be. However, a very high inlet velocity would decrease the collection efficiency because of increased turbulence and saltation/re-entrainment of particles. Kim & Lee (1990) reported that the collection efficiency is seen to increase as either the particle size or the flow rate increases, where they applied three different inlet velocities which are 8.8, 12.4 and 18.4 liter/min.

Pressure drop prediction is important as it will influence the operating cost of cyclones. As Chuah et al. (2003) cited in their report that higher inlet velocities give higher efficiencies for a given cyclone, but this also increases the pressure drop, and a trade-off must be made. They had calculated the pressure drop using 4 different empirical models such as Shepherd and Lapple (1939), Casal and Martinez (1983), Dirgo (1985), and Coker (1993) model and subsequently compare the result to experimental value made by Patterson and Munz, (1989) for the prediction under different inlet velocity.

### **2.1.3 Effect of Temperature on Cyclone Performance**

Effect of temperature on collection efficiency of cyclone is one of the most essential researches. Chen & Shi (2005) analyze this factor, where an experimental investigation on particle separation was conducted in a 300 mm diameter, tangential volute-inlet and reverse flow cyclone separator with air heated up to 973 K. They presents the experimental results on fractional as well as overall collection efficiencies of a test cyclone, aiming at better understanding the separation mechanism and improving the prediction of collection efficiencies at high temperatures which they found that at the same inlet velocity both the overall efficiency and fractional efficiency decrease with an increase of temperature.

Bohnet (1995) has measured pressure drop and the grade efficiency over the temperature range 293-1123 K since practical experience shows that the separation efficiency really obtained is mostly smaller than that calculated. A new model into which a wall friction coefficient depending on the temperature is introduced and consideration taken of the re-entrainment of already separated particles together with the boundary layer flow at the cyclone cover plate, the cyclone wall and along the outside of the vortex finder leads to measured pressure drops and grade efficiency curves for high temperatures of a high accuracy. He concluded similar to Chen & Shi where when temperature is high, the collection efficiency decrease, so as pressure drop.

#### 2.1.4 50% Particle Cut-Off Diameter

Cut-off size of particle diameter can be defined as particle size at 50% cyclone collection efficiency. The particle cut-off size  $d_{50}$  of the cyclone are always employed in the analysis of cyclone performance because its often give simple and clear indication of the particle collection efficiency of the cyclone and this makes it easy to compare the performances of cyclones under different operating conditions or of different geometrical designs. Previous experimental studies have showed that an increase in the inflow rate results in a decrease of cut size diameter (Moore & McFarland, 1990; Iozia & Leith, 1990; Zhu & Lee, 1999; and Kim & Lee, 1990). Kim & Lee (1990) observed that  $d_{50}$  is inversely proportional to inlet velocity of cyclone. As the inlet flow rate increase the collection efficiency curve become sharper, means smaller  $d_{50}$ . According to them, this is because at given flow rate it is possible to alter particle cut size diameter without deteriorating the sharpness simply by adjusting the exit tube size.

Kim et al. (2001) whose studied on virtual cyclone (minor flow pumped out at the bottom) found that compared to conventional cyclone, virtual cyclone showed smaller 50% cut-off diameter under the same operational condition. Subsequently, they correlate that pressure drop is more dependent to inlet flow compared to  $d_{50}$ , Chuah et al. (2005) made a CFD prediction of  $d_{50}$  using two different turbulence model, k- $\epsilon$  and RSM, and they demonstrated that RSM turbulence model is more accurate method of modeling the 50% cut off diameter with average deviation of about 2.1% of the measured value compared to 4.9% of RNG k- $\epsilon$ .

### **2.1.5 Review on Experimental and Simulation Studies on Cyclone Performance**

The need to enhance cyclone performance has surged since the early 40's. Due to limitation of technology, scientist need to built cyclone prototype in order to understand the influential parameters toward cyclone performance, which prove costly and time consuming. Nowadays, computer and software technology bloom enables researchers to simulate the dynamic model of cyclone, for example using Computational Fluid Dynamic (CFD) software. Table 2.1 show the summary of experimental and simulation study made by several researchers.

| N u. | Author                | Modelling CFD                                    |                              |                       |                                 |                                 | Experiments |             |                       |                     |                            | Remarks  |
|------|-----------------------|--|------------------------------|-----------------------|---------------------------------|---------------------------------|-------------|-------------|-----------------------|---------------------|----------------------------|--|
|      |                       | Turbulence                                       | Temperature                  | Collection Efficiency | Pressure Difference             | Particle Size Distribution      | Turbulence  | Temperature | Collection Efficiency | Pressure Difference | Particle Size Distribution |  |
| 1    | Chuah et al. (2006)   | Yes<br>Renault Stress Model (RSM),<br>RNG<br>K-ε | No                           | Yes                   | Yes                             | Yes                             | No          | No          | No                    | No                  | No                         | RSM turbulence model predict cyclone collection efficiency better than RNG k- ε.<br><br>Smaller cone diameter result in higher collection efficiency |
| 2    | Bohnet (1995)         | No   | No                           | No                    | No                              | No                              | No          | Yes         | No                    | Yes                 | Yes<br>Light Scattering    | High temperature separation efficiency smaller.<br><br>High temperature, small pressure difference.  |
| 3    | Altmeyer et al.(2004) | No   | Yes<br>Leith and Licht model | Yes                   | Yes<br>Mothes and Löffler model | Yes<br>Mothes and Löffler model | No          | No          | No                    | No                  | No                         | Studies of literature cases show that models used predict pretty well the experimental results.  |

| Nu | Author                | Modelling CFD |             |                       |                     |                            | Experiments |                          |                                  |                                  |                            | Remarks   |
|----|-----------------------|---------------|-------------|-----------------------|---------------------|----------------------------|-------------|--------------------------|----------------------------------|----------------------------------|----------------------------|---|
|    |                       | Turbulence    | Temperature | Collection Efficiency | Pressure Difference | Particle Size Distribution | Turbulence  | Temperature              | Collection Efficiency            | Pressure Difference              | Particle Size Distribution |   |
| 4  | Fassani et al. (2000) | No            | No          | No                    | No                  | No                         | No          | No                       | Yes<br>Function of solid loading | Yes<br>Function of solid loading | No                         | <p>The introduction of solid particles in the gas flow brought about a reduction in the cyclone pressure drop</p> <p>Pressure drop essentially did not vary as a function of solid loading</p> <p>Increasing separation efficiency With high concentration of solid loading</p> |
| 5  | Chen et al. (2003)    | No            | No          | No                    | No                  | No                         | No          | Yes                      | Yes<br>Function of temperature   | No                               | Yes                        | <p>The overall collection efficiencies of a cyclone decreases with increase in temperatures.</p> <p>The critical particle size below which the fractional efficiency increases as the particle size decreases</p>   |
| 6  | Reijnen et al. (1984) | No            | No          | No                    | No                  | No                         | No          | Yes<br>HTHP Gas Cleaning | Yes                              | Yes<br>HTHP Gas Cleaning         | No                         | Review of gas cleaning method to be used as particulate remover   |

| Nu | Author                 | Modelling CFD  |             |                       |                     |                                    | Experiments                            |             |                       |  |   | Remarks  |
|----|------------------------|--|-------------|-----------------------|---------------------|------------------------------------|--|-------------|-----------------------|--|---|--|
|    |                        | Turbulence   | Temperature | Collection Efficiency | Pressure Difference | Particle Size Distribution         | Turbulence                             | Temperature | Collection Efficiency | Pressure Difference                    | Particle Size Distribution                                    |  |
| 7  | Wang et al. (2005)     | No   | No          | No                    | No                  | No                                 | Yes<br>Laser Doppler Velocimetry (LDV) | No          | Yes                   | Yes<br>Laser Doppler Velocimetry (LDV) | No  | Insertion of a stick into the cyclone separator forms a flow wake region that decreases the tangential velocity, and increases the RMS velocity and turbulence intensity.  |
| 8  | Obermair et al. (2003) | No   | No          | No                    | No                  | No                                 | Yes<br>LDA velocity measurements       | No          | Yes                   | No                                     | No  | LDA velocity measurements of the clean gas flow of a gas cyclone with three different dust outlet geometries show that both the flow in the dust outlet geometry and the flow within the lower part of the cyclone change with outlet geometry |
| 9  | Gimbun et al. (2005)   | Yes<br>Renault Stress Model (RSM), RNG k- $\epsilon$ | No          | Yes                   | No                  | Yes<br>Cut-off diameter prediction | No                                     | No          | No                    | No                                     | No  | The Li and Wang model and CFD code both predict very well the cyclone efficiency and cut-off size for any operational conditions   |
| 10 | Kim and Lee (1990)     | No   | No          | No                    | No                  | No                                 | No                                     | No          | Yes                   | Yes<br>Exit tube size effect           | Yes<br>50% cut-off diameter in the function of exit tube size | Exit tube size effect cyclone performance significantly  |



| Nu | Author                  | Modelling CFD                                    |             |   |  |                            | Experiments |             |                                     |                     |                                     | Remarks   |
|----|-------------------------|--|-------------|---|--|----------------------------|-------------|-------------|-------------------------------------|---------------------|-------------------------------------|---|
|    |                         | Turbulence                                       | Temperature | Collection Efficiency                       | Pressure Difference                              | Particle Size Distribution | Turbulence  | Temperature | Collection Efficiency               | Pressure Difference | Particle Size Distribution          |   |
| 11 | Kim et al. (2001)       | No   | No          | No  | No   | No                         | No          | No          | Yes                                 | Yes                 | Yes<br>Cut-off diameter             | Comparison between conventional and virtual cyclone performance<br><br>Virtual cyclone has minor flow pumped out at bottom                      |
| 12 | Hu and McFarland (2007) | Yes<br>RSM with high scheme discretization phase | No          | Yes<br>Lagrangian discrete phase model, DPM | Yes<br>RSM with high scheme discretization phase | No                         | No          | No          | Yes                                 | Yes                 | Yes                                 | CFD program Fluent, using RSM and DPM with suitable discretization schemes, was found to properly predict particle collection and pressure drop |
| 13 | Tsai et al. (2004)      | No   | No          | No  | No   | No                         | No          | No          | Yes<br>Function of cyclone pressure | No                  | Yes<br>Cut-off aerodynamic diameter | Pressure inside the cyclone was found to have a considerable effect on the particle collection efficiency                                       |

Table 2.1: Review on Experimental and Simulation Researches

## **2.2 Uses of Cyclone Separation**

### **2.2.1 Cyclone Gasifier in Biomass Plant**

Electricity generated from biomass is a great alternative replacing fossil fuels where it promise high efficiency electricity production and low emissions and at competitive cost if the biomass fuel is available at low cost. Gas turbine initially designed to be used in clean air environment, but biomass fuel consists of relatively high ash content where ash tends to form compound with negative effect to plant hardware. In Europe research has been made in order to find a way to clean up the gas producer from biomass waste. Most of this research is using Fluidized Bed Gasifier (FBG) that include extensive gas cleaning and high capital investment. In a gas turbine plant, cyclone gasifier has been design in to replace FBG. The cyclone gasifier was more reliable than traditional fluidized bed gasifiers due to its simplicity and capability to cope well with unpredictable variation in its operating environment with minimal damage, alteration or loss of functionality. The cyclone gasifier fading the necessity of complex hot gas clean up which reduces system efficiency especially for small plant.

Syred et. al. (2004) stated that cyclone gasifier was a good ash separator, removes significant quantities of alkalis and enable larger size of fuel particles to be used with size distribution extending from 2 to 3 mm. Syred et. al. (2004) has developed an inverted cyclone gasifier coupled to a cyclone combustor in series for indirect firing of a small scale gas turbine. The cyclone gasifier is capable of efficient gasification, with hot gas clean up, alkali separation and particle removal incorporated into the system by means of cyclone technology and vortex collector pocket (VCP). Exhaust gas is then fired into secondary cyclone combustor capable of burning variety of fuels with varying calorific value for firing small gas turbines (less than 2 MW).

### 2.2.2 Hydro-Cyclone Separation

Aerocyclone separation is meant to separate particles of solid and gas phase while hydrocyclone was created to separate particles in a liquid suspension based on particles density. A hydrocyclone may be used to separate solids from liquids or to separate liquids of different density. The shape is similar to conventional aerocyclone, normally have a cylindrical section at the top where liquid is being fed tangentially, and a conical base. The angle, and hence length of the conical section, plays a role in determining operating characteristics. Internally, centrifugal force is countered by the resistance of the liquid, with the effect that larger or denser particles are transported to the wall for eventual exit at the *reject* side with a limited amount of liquid, whilst the finer, or less dense particles, remain in the liquid and exit at the overflow side through a tube extending slightly into the body of the cyclone at the center

Forward hydrocyclones remove particles that are denser than the surrounding fluid, while reverse hydrocyclones remove particles that are less dense than the surrounding fluid. In a reverse hydrocyclone the overflow is at the apex and the underflow at the base. There are also parallel-flow hydrocyclones where both the *accept* and *reject* are removed at the apex. Parallel-flow hydrocyclones remove particles that are lighter than the surround fluid.

In a suspension of particles with the same density, a relatively sharp cut can be made. The size at which the particles separate is a function of cyclone diameter, exit dimensions, feed pressure and the relative characteristics of the particles and the liquid. Efficiency of separation is a function of the solids' concentration: the higher the concentration, the lower the efficiency of separation. There is also a significant difference in suspension density between the base exit (fines) and the apex exit, where there is little liquid flow. If the size range of the particles is limited, but there are differences in density between types of particles, the denser particles will

exit preferentially at the apex. The device is therefore a means of selective concentration of, for example, minerals. Recent studies made by Yoshida et al. (2008) where the effect of the multi-inlet flow injection method of hydrocyclones on particle separation performance was examined. They found that cyclone with two inlets flow indicated high collection efficiency and sharp separation performance compared to the standard cyclone while cyclone with a small additional flow injection area showed a smaller cut size as the flow rate of the additional flow increased.

Hydrocyclone can be found in pulp and paper mills to remove sand, staples, plastic particles and other contaminants, and also popular in the drilling industry to separate sand from the expensive clay that is used for lubrication during the drilling. Also in the mining industry hydro-cyclone is used to separate coarse tailings from the fine fraction to obtain good material for tailings dam construction.

### **2.2.3 Circulating Fluidized Bed (CFB) Reactor**

In the past cyclones were considered as low efficiencies separator, but advanced design principles have significantly improved their efficiency, now in excess of 98% at ambient operating conditions for particle sizes larger than approximately  $5\mu\text{m}$  when these principles were implement to. The cyclones associated with CFB reactors are operating within a wide variety of temperatures and pressures and are subject to a very high solids loading due to the applied solids circulation rate (Velden et al., 2007). The main part of the CFB is formed by the vertical riser where the reaction between solids and gas takes place. The gas–solid suspension leaves the riser at the top and enters a cyclone which separates the gas from the solids. The latter are recycled to the riser through the downcomer and are re-introduced in the riser by means of a mechanical or a non-mechanical valve. It is of the utmost importance for the cyclone to separate the solids very efficiently to avoid the loss of solid reactants or catalyst.

## CHAPTER 3

### RESEARCH METHODOLOGY

#### 3.0 Introduction

Cyclones are devices that employ a centrifugal force generated by a spinning gas stream to separate particles from the carrier gas. Separation efficiencies of cyclones can be very high for particle size larger than  $5\mu\text{m}$ , can be operated at very high gas loading, and well suited for operation at extreme temperature and pressure. Cyclone performance from the eye of an engineer means two parameters, collection efficiency and pressure drop across the cyclone. Optimum cyclone separation can be achieved if cyclone collection efficiency accurately predicted.

CFD is an acronym for Computational Fluid Dynamics, or the art of using a computer to predict how gases and liquids flow. CFD has a great potential to predict the flow field characteristics and particle trajectories inside the cyclone as well as the pressure drop (Griffith & Boysan, 1996). The numerical techniques and turbulence models that employed in CFD is capable to solve the complicated swirling turbulence flow in cyclone. Cyclone simulation began in 1982, with pioneering work of Boysan et al. which used an axis symmetry model and a hybrid model of turbulence composed of a combination of the k-s model and the algebraic stress model. After that, Pericleous (1987) presented a new axis-symmetry model with turbulence prediction which included the simplification of Prandtl's mixture length theory to simulate hydrocyclones. Duggins and Frith (1987) presented the failures of the k- $\epsilon$  model in simulating swirling flows and proposed a new turbulence model using a combination of the k-s model and the mixture length model to introduce the anisotropic behavior of the Reynolds stress. Madsen et al. (1994), using a version of the algebraic stress model of turbulence, presented a new simulation of cyclones,

solving the gas phase by the Flow-3D computational code e developing the Lagrangian model for the particles. Meier and Mori (1996), presented a new model of turbulence of the gas phase considering the anisotropic behavior of the Reynolds stress by using a combination between the  $k-\varepsilon$  model and the mixture length theory of Prandtl. The results were validated by four test cases from the literature and proved to be satisfactory.

This study represents the prediction of miniature aero-cyclone collection efficiency, pressure drops and 50% particle cut-off diameter using CFD simulation. At the same time, the influence of exit tube dimension, turbulence models and inlet velocity toward these three parameters will be concluded based on the CFD prediction. Finally these prediction data will be verified with experimental data found from literature.

### 3.1 CFD Modelling Approach

#### 3.1.1 Simulation Procedure

Basically there are 6 steps that need to be followed in order to achieve the objectives of this study. Flow chart below shows the simulation procedures and followed by thorough explanation of each steps.

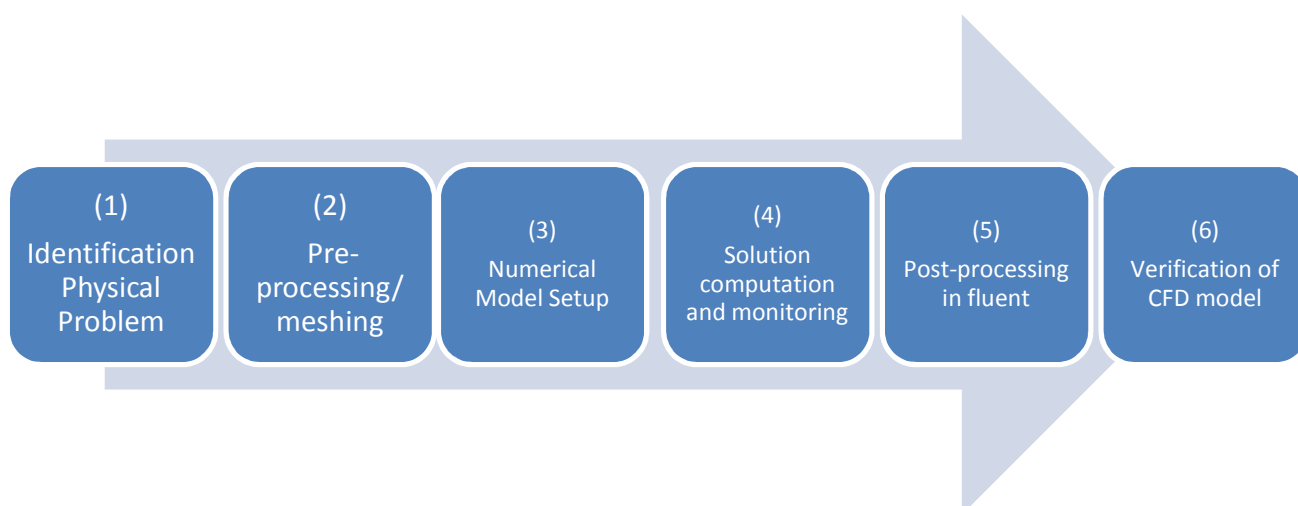


Figure 3.1: Steps for CFD Modelling

### **3.1.1.1 Identification of Physical Problem**

This is the very first step of CFD simulation where modeling goals were defined. In the end of this study, the results we were looking for are the collection efficiency, pressure drop across the cyclone and the 50% cut-off particle diameter where these parameters shall define the cyclone performance. At this initial stage, physical model that will need to be included in the analysis was decided, where the complex swirling flow inside the cyclone demanded turbulence model to be implemented in this simulation. Simplifying assumption needed in the simulation was made, where in order to enable Discrete Phase Modeling (DPM), the particle is assumed to be sphere. Complex modeling sometimes require unique modeling capability, for example user define function (written in C) in Fluent 6.0. The degree of accuracy and simulation estimated duration was also decided at this early stage. The cyclone model configuration is based on Kim & Lee (1990) experimental cyclone prototype.

### **3.1.1.2 Pre-processing/meshing**

The partial differential equations that govern fluid flow and heat transfer are not usually amenable to analytical solutions, except for very simple cases. Therefore, in order to analyze fluid flows, flow domains are split into smaller subdomains (made up of geometric primitives like hexahedra and tetrahedral in 3D and quadrilaterals and triangles in 2D). The governing equations are then discretized and solved inside each of these subdomains. Typically, one of three methods is used to solve the approximate version of the system of equations: finite volumes, finite elements, or finite differences. The subdomains are often called elements or cells, and the collection of all elements or cells is called a mesh or grid. The origin of the term mesh (or grid) goes back to early days of CFD when most analyses were 2D in nature. For 2D analyses, a domain split into elements resembles a wire mesh, hence the name.

The process of obtaining an appropriate mesh (or grid) is termed mesh generation (or grid generation), and has long been considered a bottleneck in the analysis process due to the lack of a fully automatic mesh generation procedure. Specialized software programs have been developed for the purpose of mesh and grid generation, and access to a good software package and expertise in using this software are vital to the success of a modeling effort. Gambit 2.0 software was used to mesh the cyclone models, where the grid generated was coarse with 36,000 cells, as shown in figure 3.2..

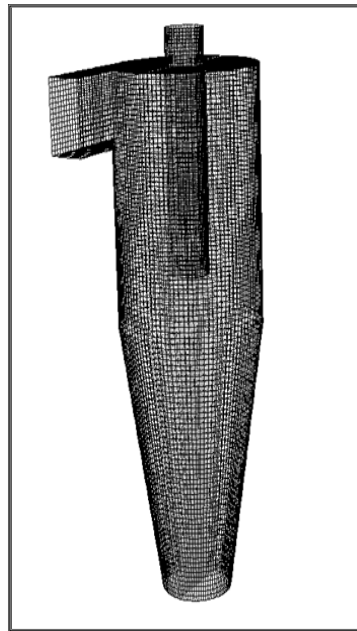


Figure 3.2: Coarse grid cyclone mesh



### 3.1.1.3 Numerical Model Setup

Numerical model need to be setup before it is solved. In this study the appropriate physical model chosen is turbulence model (RSM & DES). Material that is injected through inlet is define as mixture, which is actually dioctyl plathlate (DOP) with density  $980 \text{ kg/m}^3$  that enter the cyclone with air.

Boundary conditions specify the flow and thermal variables on the boundaries of physical model. They are, therefore, a critical component of FLUENT simulations and it is important that they are specified appropriately. The boundary types that were set for this experiment are as follow:

- Inlet set as velocity inlet
- Outlet top set as particle escaped
- Outlet bottom set as particle trap
- Cyclone wall set as standard wall function

Three different air flow rate is set for this experiment in order to observe the influence of velocity inlet toward cyclone performance. The flow rate chosen by Kim & Lee (1990) are 8.8, 12.4 and 18.4 liter/min. At last the solver control is setup and convergence monitor is fixed into the screen, letting knows that the model is ready for solution computation.

### 3.1.1.4 Solution Computation & Monitoring

After boundary condition has been set, solution is numerically computed by the software. The discretized conservation equation is solved iteratively. A number of iterations are usually required to reach a converged solution. Convergence is reach when changes in solution variables from one iteration to next are negligible and the overall property conservation is achieved. The residual will provide a mechanism to help monitor this trend. The accuracy of converged

solution is dependent on appropriateness and accuracy of physical model, grid resolution and independence, and problem setup.

### **3.1.1.5 Post-processing in Fluent**

At this stage, the result is examined to review the solution and extract the useful data. The data examination is meant to ensure the property conservation and correct physical behavior. High residual may be attributable to only a few cells of poor quality. The collection efficiency data is extracted using particle track function in fluent. Number of particle trapped in out bottom is divided to total particle tracked at inlet and times by 100 are the correct way to extract collection efficiency data.

$$\text{Collection Efficiency} = \frac{\text{number of particle trapped at bottom}}{\text{number of particle tracked at inlet}} \times 100\%$$

The collection efficiency data is extracted at various particle diameters ranging from 1-10  $\mu\text{m}$  so collection efficiency versus particle diameter can be built. From that curve, 50% cut-off diameter data is extracted, 50% cut-off diameter,  $d_{50}$  is the particle size at 50% collection efficiency. The pressure drop can be determined by displaying static pressure profile at contour function. The cursor is clicked at inlet point and outlet top point, where pressure of both point will appear in the screen. Simple manual subtraction will yield pressure drop across the cyclone.

### **3.1.1.6 Verification of CFD model**

The final stage of this study requires verification of simulation data with experimental data collected from literature. In this case, Kim & Lee (1990) experimental data for cyclone I & II are chosen for verification. Comparison of simulation data with experimental data will

determine the accurateness of CFD prediction, where deviation less than 10% is considered satisfactory.

### 3.1.2 Cyclone Design

CFD simulation can only be operated with completely meshed miniature cyclone design. The cyclone simulated in this study is based on Kim and Lee (1990) miniature cyclone specification. Two cyclones were used in this study which only differs on the exit tube diameters, so the effect of vortex finder dimension can be analyze. Three different flow rates is chosen by Kim and Lee (1990) in their experiment, which are 8.8, 12.4 and 18.4 liter/min. These flow rates are also utilized in this simulation in order to observe influence of inlet velocity toward cyclone performance. Material chosen for this simulation is dioctyl phlatlate (DOP) with density  $980 \text{ kg/m}^3$ . DOP enter the cyclone with air, some of it collected at bottom trap while others escaped at top of the cyclone. Table 1 shows the configuration of Kim and Lee (1990) cyclone.

| Cyclone | Dimensions (cm)      |                           |      |      |     |     |     |     |
|---------|----------------------|---------------------------|------|------|-----|-----|-----|-----|
|         | Body Diameter, $D_B$ | Exit Tube Diameter, $D_E$ | X    | Y    | S   | h   | H   | B   |
| I       | 3.11                 | 0.8                       | 0.71 | 1.29 | 3.6 | 4.5 | 9.5 | 1.5 |
| II      | 3.11                 | 1.36                      | 0.71 | 1.29 | 3.6 | 4.5 | 9.5 | 1.5 |

**Table 3.1: Dimensions of Tested Cyclones**

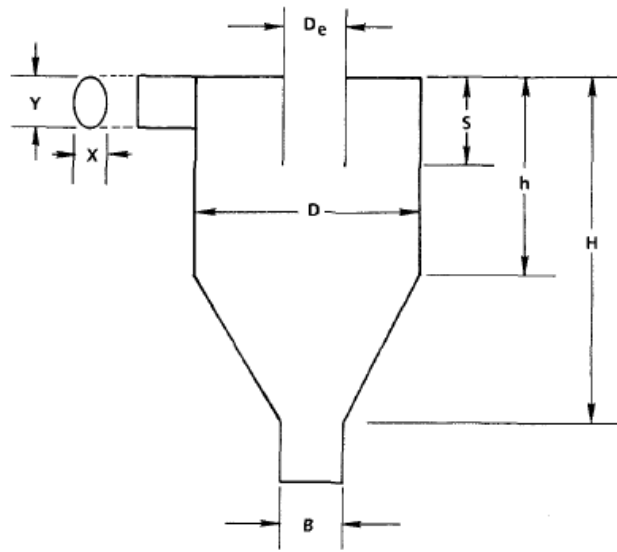


Figure 3.3: Cyclone Dimension

### 3.4 Numerical Modeling of the Cyclone

The miniature cyclone is simulated using software Fluent 6.5, that is available in workstation in Process Control Lab of Universiti Malaysia Pahang (UMP). FLUENT software is sophisticated numerics and robust solvers including a pressure-based coupled solver, a fully-segregated pressure-based solver and two density-based solver formulations which help ensure robust and accurate results for a nearly limitless range of flows. Advanced parallel processing numerics can efficiently utilize multiple, multi-core processors in a single machine and in multiple machines on a network. Dynamic load balancing automatically detects and analyzes parallel performance and adjusts the distribution of computational cells among the processors so that a balanced load is shared by the CPUs even when complex physical models are in use. According to Gimbut et al. (2005) the conservation of mass, momentum and energy in a fluid flow are expressed in terms of non-linear partial differential equations that generally defy solution by analytical means. The solution of these equations has been made possible by the advent of powerful workstations, opening avenues towards the calculation of complicated flow fields with relative ease.

Griffiths and Boysan (1996) state that for the turbulent flow in a cyclone the key to the success of CFD lies with the accurate description of the turbulent behavior of the flow. There are several turbulence models available in Fluent that are capable to generate swirling flow in a cyclone, ranging from industrial standard RNG k- $\epsilon$  to more advanced model such as Reynold Stress Model (RSM) and Detached Eddy Simulation (DES). For this study, two advanced model, RSM and DES are chosen due to its capability and accuracy in predicting swirling motion of particle inside a cyclone. At the end of the simulation, the prediction data made by these two models are compared to distinguish each models performance.

### **3.4.1 Governing Equation for Fluid Flow inside a Cyclone**

Fluid flows have long been mathematically described by a set of nonlinear, partial differential equations, namely the Navier-Stokes equations, but, except in a few simple situations, theoretical solutions to the Navier-Stokes equations are still very difficult to find. Even with the advent of the modern digital computers, direct numerical solutions to the Navier-Stokes equations for the fluid flow of engineering interest is still not easy. A practical way of simulating fluid flows in engineering applications is to use turbulence models and solve for the mean fluid velocity and pressure.

It is important to note that most fluid flows in cyclones operate in the turbulent fluid flow regime, whilst some small cyclones may well be operated in the transition flow regime where fluid flow structures are different from those which exist in a fully developed turbulent flow and therefore different procedures may be employed for the modelling of the transition flow.

However, the problem has been limited to a discussion of fully developed turbulent fluid flows in cyclones. For the steady and incompressible fluid flow in cyclones, the following Reynolds-averaged Navier-Stokes equations are employed:

*Navier-Stokes Equation*

$$\rho u^j \frac{\partial u^i}{\partial x^j} = - \frac{\partial p}{\partial x^i} + \frac{\partial}{\partial x^j} \left[ \mu \left( \frac{\partial u^i}{\partial x^j} + \frac{\partial u^j}{\partial x^i} \right) \right] + \frac{\partial \tau^{ij}}{\partial x^j} \quad (1)$$

*Continuity Equation*

$$\frac{\partial u^i}{\partial x^i} = 0 \quad (2)$$

where the superscripts  $i, j = 1, 2, 3$  indicate the components in the Cartesian co-ordinate system,  $u^i, p, \rho$  and  $\mu$  are the fluid velocity, pressure, density and molecular viscosity, respectively, and

$$\tau^{ij} = -\overline{\rho u'^i u'^j} \quad (3)$$

is known as the Reynolds stress tensor which represents the effects of the turbulent fluctuations on the fluid flow. The overbar represents a Reynolds average and the dash represents the fluctuating part. For convenience, the overbars on top of the mean fluid velocity  $u^i$  and the pressure  $p$  have been removed in equations (1) and (2) and in the remainder of this paper. However, the Reynolds-averaged Navier-Stokes equations (1) and (2) are not closed unless a model is provided which ties the Reynolds stress tensor  $\tau^{ij}$  to the global history of the mean fluid velocity  $u^i$  in a physically consistent fashion.

### 3.4.2 Turbulence Model

Reynolds Stress models (RSM) solve for individual Reynolds stresses and for the turbulent dissipation  $\epsilon$ . The Reynolds Stress model assumes that the factors within it contain no dependence on the Reynolds number of the flow. However it should be noted that this is not always true especially at moderate Reynolds numbers. The central concept of the Reynolds stress model is that the stress tensor  $R_{ij}$  is determined locally within the cell. The Reynolds Stress turbulence model yields an accurate prediction of swirl flow pattern, axial velocity, tangential velocity and pressure drop on cyclone simulations (Reddy, 2003; Fraser, 2003; Fredriksson, 1999).

The Reynolds stress model involves calculation of the individual Reynolds stresses,  $\overline{\rho u^i u^j}$ , using differential transport equations. The individual Reynolds stresses are then used to obtain closure of the Reynolds-averaged momentum equation. The exact transport equations for the transport of the Reynolds stresses  $\overline{u_i' u_j'}$  may be written as follows:

$$\begin{aligned} \underbrace{\frac{\partial}{\partial t} (\overline{\rho u_i' u_j'})}_{\text{Time derivative}} + \underbrace{\frac{\partial}{\partial x_k} (\overline{\rho u_k u_i' u_j'})}_{C_{ij}=\text{Convection}} = & - \underbrace{\frac{\partial}{\partial x_k} [\overline{\rho u_i' u_j' u_k'} + \overline{p(\delta_{kj} u_i' + \delta_{ik} u_j')}]}_{D_{T,ij}=\text{Turbulent diffusion}} + \underbrace{\frac{\partial}{\partial x_k} \left[ \mu \frac{\partial}{\partial x_k} (\overline{u_i' u_j'}) \right]}_{D_{L,ij}=\text{Molecular diffusion}} \\ & - \underbrace{\rho \left( \overline{u_i' u_k'} \frac{\partial u_j}{\partial x_k} + \overline{u_j' u_k'} \frac{\partial u_i}{\partial x_k} \right)}_{P_{ij}=\text{Stress production}} + \underbrace{\frac{p}{\rho} \left( \frac{\partial u_i'}{\partial x_j} + \frac{\partial u_j'}{\partial x_i} \right)}_{\phi_{ij}=\text{Pressure strain}} - \underbrace{2\mu \frac{\partial u_i'}{\partial x_k} \frac{\partial u_i'}{\partial x_k}}_{\varepsilon_{ij}=\text{Dissipation}} \\ & - \underbrace{2\rho \Omega_k (\overline{u_j' u_m'} \varepsilon_{ikm} + \overline{u_i' u_m'} \varepsilon_{jkm})}_{F_{ij}=\text{Production by system rotation}} \end{aligned}$$

The  $\Omega_k$  is an angular velocity and both  $\varepsilon_{ikm}$  and  $\varepsilon_{jkm}$  are permutation tensors. Of the various terms in these exact equations,  $C_{ij}$ ,  $D_{L,ij}$ ,  $P_{ij}$ , and  $F_{ij}$  do not require any modelling. However,  $D_{T,ij}$ ,  $\phi_{ij}$ , and  $\varepsilon_{ij}$  need to be modelled to close the equations. The reason is simply because the averaging procedure of  $\overline{u_i' u_j' u_k'}$  will generate a lot of unknown variables and it becomes impossible to solve them directly.

The turbulent diffusivity transport term is modelled using a simplified form of the generalised gradient diffusion hypothesis as:

$$D_{T,ij} = \frac{\partial}{\partial x_k} \left[ \frac{\mu_t}{\sigma_k} \frac{\partial (\overline{u_i' u_j'})}{\partial x_k} \right]$$

The pressure strain term is modelled as:

$$\phi_{ij} = \frac{p}{\rho} \left( \frac{\partial u_i'}{\partial x_j} + \frac{\partial u_j'}{\partial x_i} \right) = -C_1 \frac{\varepsilon}{k} \left[ \overline{u_i' u_j'} - \frac{2}{3} \delta_{ij} k \right] - C_2 \left[ P_{ij} - \frac{2}{3} \delta_{ij} P \right]$$

where  $P = 0.5P_{ij}$  is the turbulence production due to shear, and the constants are  $C_1 = 1.8$  and

$$C_2 = 0.6.$$

The dissipation term is assumed to be isotropic and is approximated by:

$$\varepsilon_{ij} = 2\mu \frac{\overline{\partial u'_i}}{\partial x_k} \frac{\overline{\partial u'_i}}{\partial x_k} = \frac{2}{3} \delta_{ij} \varepsilon$$

The scalar dissipation rate is computed with a model transport equation similar to the one in the standard  $k$ - $\varepsilon$  model.

The difficulties associated with the use of the standard LES models, particularly in near-wall regions, has lead to the development of hybrid models that attempt to combine the best aspects of RANS and LES methodologies in a single solution strategy. An example of a hybrid technique is the DES (Spalart et al., 1997) approach. This model attempts to treat near-wall regions in a RANS-like manner, and treat the rest of the flow in an LES-like manner. The model was originally formulated by replacing the distance function  $d$  in the Spalart-Allmaras (S-A) model with a modified distance function.

The SA one-equation model solves a single partial differential equation for a variable  $\tilde{\nu}$  which is related to the turbulent viscosity. The variable  $\tilde{\nu}$  is identical to the turbulent kinematic viscosity except in the near-wall (viscous-affected) region. The model includes a wall destruction term that reduces the turbulent viscosity in the log layer and laminar sub-layer. The transport equation for DES is:

$$\frac{\partial}{\partial t}(\rho\tilde{\nu}) + \frac{\partial}{\partial x_i}(\rho\tilde{\nu}u_i) = G_v + \frac{1}{\sigma_{\tilde{\nu}}} \left[ \frac{\partial}{\partial x_j} \left\{ (\mu + \rho\tilde{\nu}) \frac{\partial \tilde{\nu}}{\partial x_j} \right\} + C_{b2}\rho \left( \frac{\partial \tilde{\nu}}{\partial x_j} \right)^2 \right] - Y_v$$

The turbulent viscosity is determined via:

$$\mu_t = \rho\tilde{\nu}f_{v1}, \quad f_{v1} = \frac{\chi^3}{\chi^3 + C_{v1}^3}, \quad \chi \equiv \frac{\tilde{\nu}}{\nu}$$

where  $\nu = \mu / \rho$  is the molecular kinematic viscosity. The production term,  $G_v$ , is modelled as:



$$G_v = C_{b1} \rho \tilde{S} \tilde{v}, \quad \tilde{S} \equiv S + \frac{\tilde{v}}{k^2 d^2} f_{v2}, \quad f_{v2} = 1 - \frac{\chi}{1 + \chi f_{v1}}$$

$S$  is a scalar measure of the deformation rate tensor which is based on the vorticity magnitude in the SA model. The destruction term is modelled as:

$$Y_v = C_{w1} \rho f_w \left( \frac{\tilde{v}}{d} \right)^2, \quad f_w = g \left[ \frac{1 + C_{w3}^6}{g^6 + C_{w3}^6} \right]^{1/6}, \quad g = r + C_{w2} (r^6 - r), \quad r \equiv \frac{\tilde{v}}{\tilde{S} k^2 d^2} \quad (4)$$

The closure coefficients for SA model **Error! Reference source not found.** are  $C_{b1} = 0.1355$ ,

$$C_{b2} = 0.622, \quad \sigma_{\tilde{v}} = \frac{2}{3}, \quad C_{v1} = 7.1, \quad C_{w1} = \frac{C_{b1}}{k^2} + \frac{(1 + C_{b2})}{\sigma_{\tilde{v}}}, \quad C_{w2} = 0.3, \quad C_{w3} = 2.0, \quad k = 0.4187.$$

In the SA model the destruction term (eq. 4) is proportional to  $(\tilde{v}/d)^2$ . When this term is balanced with the production term, the eddy viscosity becomes proportional to  $\tilde{S} d^2$ . The Smagorinsky LES model varies its sub-grid-scale (SGS) turbulent viscosity with the local strain rate, and the grid spacing is described by  $\nu_{SGS} \propto \tilde{S} \Delta^2$  where  $\Delta = \max(\Delta x, \Delta y, \Delta z)$ . If  $d$  is replaced with  $\Delta$  in the wall destruction term, the SA model will act like a LES model. To exhibit both RANS and LES behaviour,  $d$  in the SA model is replaced by:

$$\tilde{d} = \min(d, C_{des} \Delta)$$

where  $C_{des}$  is a constant with a value of 0.65. Then the distance to the closest wall  $d$  in the SA model is replaced with the new length scale  $\tilde{d}$  to obtain the DES. The purpose of using this new length is that in boundary layers where  $\Delta$  far exceeds  $d$ , then the standard SA model applies since  $\tilde{d} = d$ . Away from walls where  $\tilde{d} = C_{des} \Delta$ , the model turns into a simple one equation SGS model, close to Smagorinsky's in the sense that both make the mixing length proportional to  $\Delta$ . The Smagorinsky model is the standard eddy viscosity model for LES. On the other hand, this approach retains the full sensitivity of RANS model predictions in the boundary layer. This model has never been applied to predict the stirred tank flows in the past and so this is an objective of the current study.

The finite volume method has been used to discretize the partial differential equations of the model using the SIMPLE method for pressure-velocity coupling and the Second Order Upwind scheme to interpolate the variables on the surface of the control volume. The segregated solution algorithm was selected. The Reynolds stress (RSM) turbulence model was used in this model due to the anisotropic nature of the turbulence in cyclones. Standard Fluent wall functions were applied and high order discretization schemes were also used. The simulation is then solved with a coupling of unsteady and steady state solvers in FLUENT. To calculate the trajectories of particles in the flow, the discrete phase model (DPM) was used to track individual particles through the continuum fluid.

### 3.5 Details on CFD Setting

The details of CFD simulation setting is shown in table below:

| Details                                     | Setting   |
|---|---|
| <b>Boundary Condition</b>                   |   |
| Inlet                                       | Velocity  |
| Outlet Top                                  | Outflow (particle escape)                                   |
| Outlet Bottom                               | Outflow (particle trap)                                     |
| Cyclone Wall                                | Standard wall function                                      |
| <b>Viscous</b>                              |   |
| Turbulence                                  | Reynold Stress Model (RSM)<br>Detached EddySimulation (DES) |
| <b>Discretization</b>                       |   |
| Pressure                                    | Presto!   |
| Pressure-velocity Coupling                  | 2 <sup>nd</sup> Order Upwind                                |
| Momentum                                    | 2 <sup>nd</sup> Order Upwind                                |
| Turbulence Kinetic Energy                   | 2 <sup>nd</sup> Order Upwind                                |
| Reynold Stresses                            | 2 <sup>nd</sup> Order Upwind                                |
| <b>Discrete Phase Modelling (DPM)</b>       |   |
| Assumption                                  | Sphere Particle   |
| Maximum number of Steps (phase integration) | 10000   |

Table 3.2: Details on CFD Setting

## CHAPTER 4

### RESULTS & DISCUSSION

#### 4.0 Introduction

The objectives of this study are to understand the influence of inlet velocity and exit tube dimension to miniature aerocyclone performance (collection efficiency, pressure drop) from data predicted by CFD simulation. At the same time, performance of two different turbulence model implemented in CFD can be analyzed, from view of prediction accuracy. Both turbulent models prediction accuracy can be determined by comparing simulation data with experimental data made by Kim & Lee (1990). This section will present the result obtain from simulation in the function of cyclone collection efficiency and pressure drop and result justification.

#### 4.1 Cyclone Collection Efficiency

Cyclone collection efficiency is a great indicator of cyclone performance. These mini cyclones are operated under ambient temperature where temperature change is neglected. Many applications of cyclone are operated at normal temperature such saw dust and grain dust removal from air. Kim & Lee (1990) presented their experimental data under room temperature, so the simulation is set at room temperature. There are two set of cyclone collection efficiency data presented, where both set differ only in exit tube dimension. Cyclone II has larger exit tube diameter than cyclone I, so the exit tube dimension influence on cyclone collection efficiency can be observed. The collection efficiency versus particle diameter is plotted for 3 different inlet

velocities, which are 8.8, 12.4 and 18.4 litre/min. Figure 4.1 – 4.3 shows the comparison between Kim & Lee (1990) experimental data and CFD prediction for Cyclone I ( $D_e = 0.8$  cm).

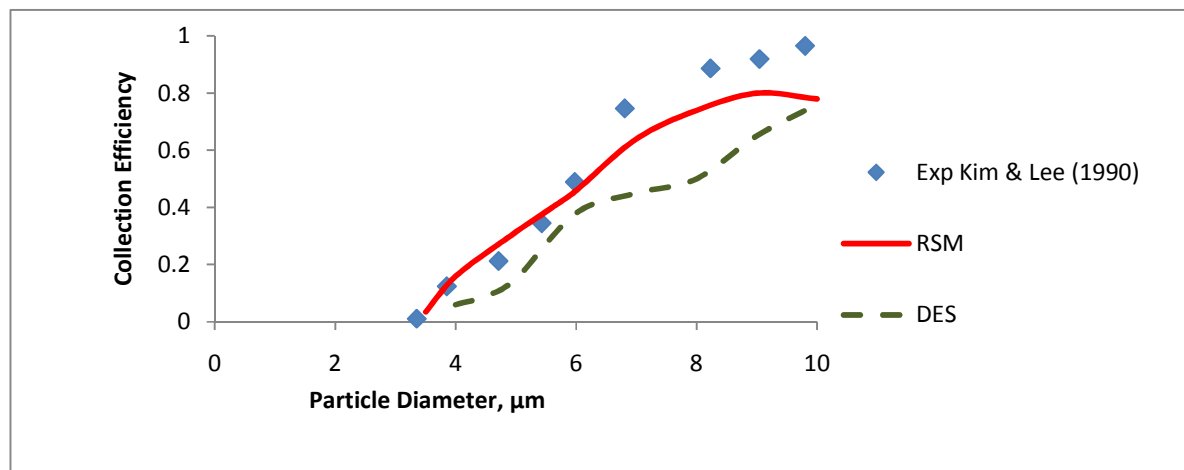


Figure 4.1: Simulated collection efficiencies for Kim & Lee cyclone I ( $P = 1$  atm,  $T = 273$  K,  $v_i = 8.8$  lpm,  $D_e = 0.8$  cm). Data point from Kim and Lee (1990).

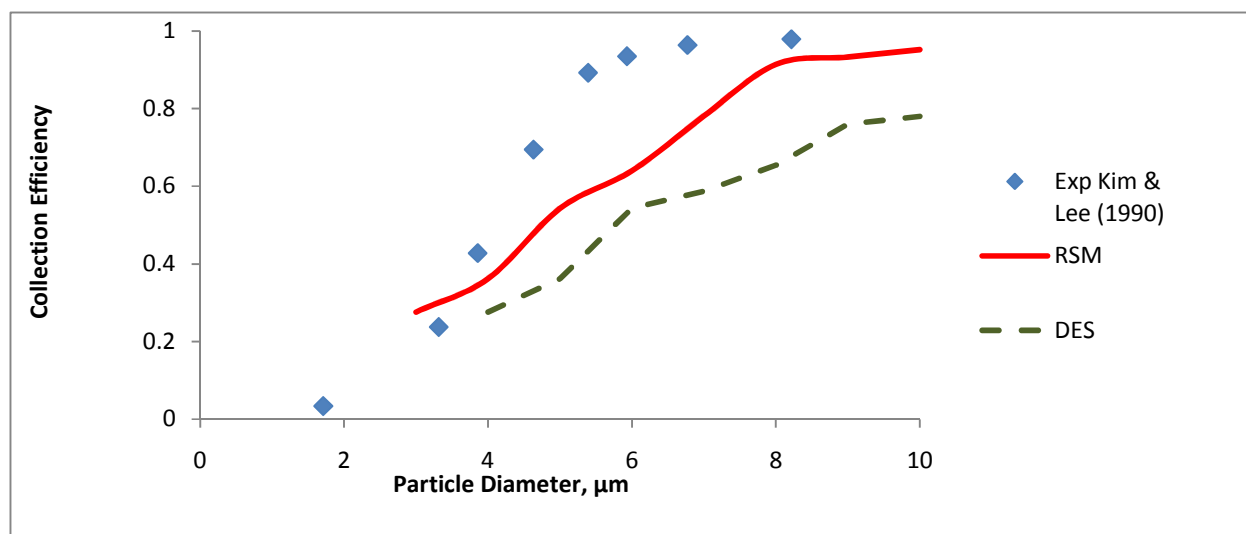


Figure 4.2: Simulated collection efficiencies for Kim & Lee cyclone I ( $P = 1$  atm,  $T = 273$  K,  $v_i = 12.4$  lpm,  $D_e = 0.8$  cm). Data point from Kim and Lee (1990).

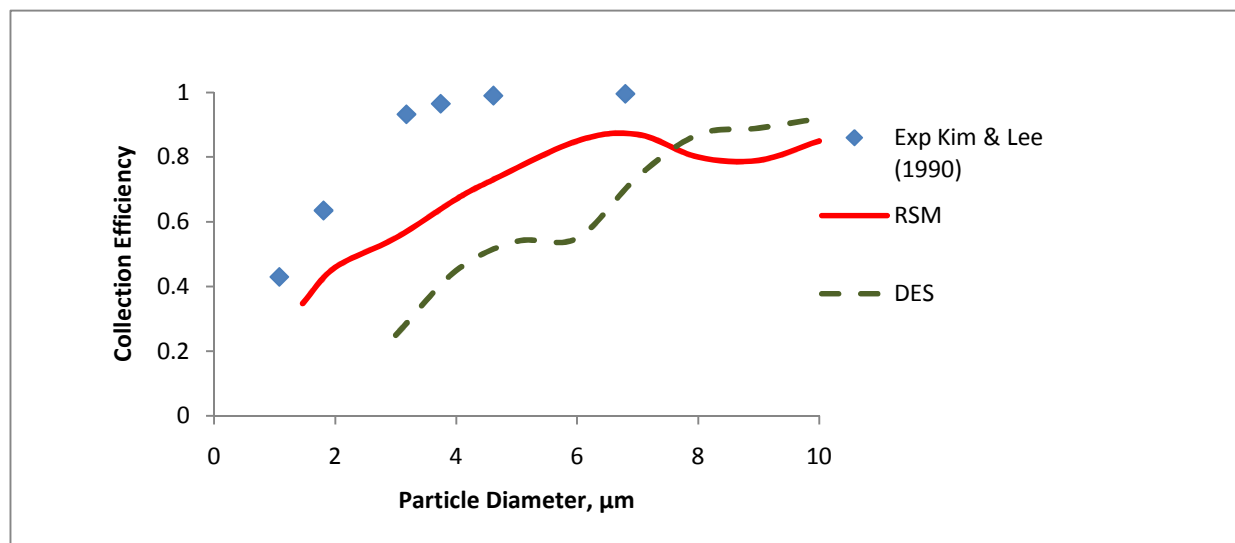


Figure 4.3: Simulated collection efficiencies for Kim & Lee cyclone I ( $P = 1$  atm,  $T = 273$  K,  $v_i = 18.4$  lpm,  $D_e = 0.8$  cm). Data point from Kim and Lee (1990).

Most of the measurement data are seen to projected a so-called “S”- shape curve, with little scatter. Early observation that can be made is the collection efficiency is seen to increase as either the particle size or flow rate increases. Figure 4.4 – 4.6 shows the comparison between Kim & Lee (1990) experimental data and CFD prediction for Cyclone II ( $D_e = 1.36$  cm).

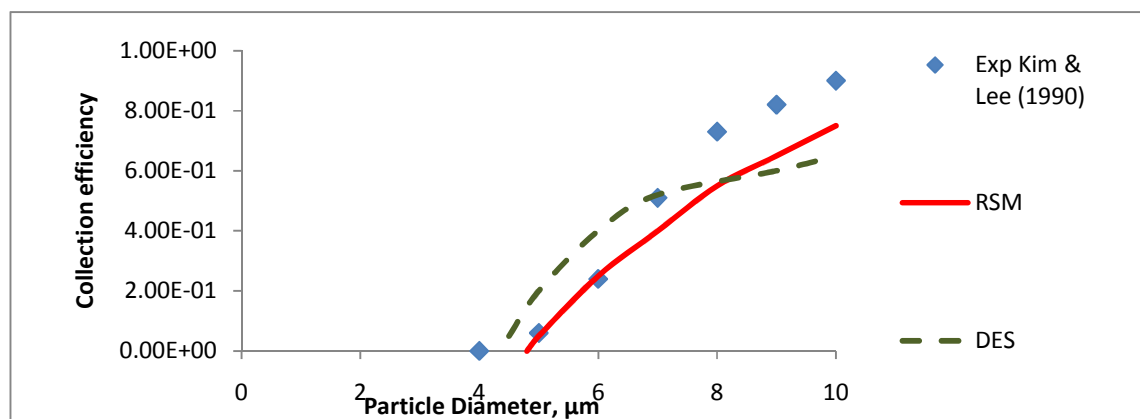


Figure 4.4: Simulated collection efficiencies for Kim & Lee cyclone II ( $P = 1$  atm,  $T = 273$  K,  $v_i = 8.8$  lpm,  $D_e = 1.36$  cm). Data point from Kim and Lee (1990).

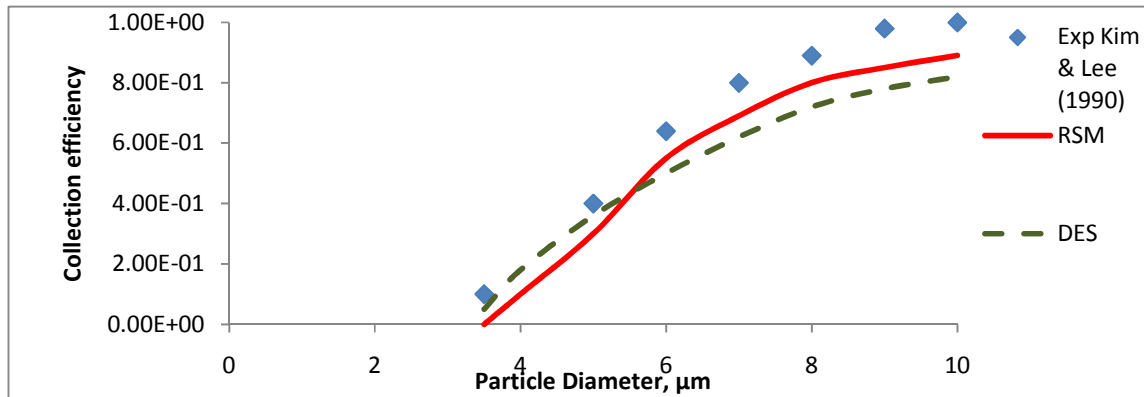


Figure 4.5: Simulated collection efficiencies for Kim & Lee cyclone II ( $P = 1$  atm,  $T = 273$  K,  $v_i = 12.4$  lpm,  $D_e = 1.36$  cm). Data point from Kim and Lee (1990).

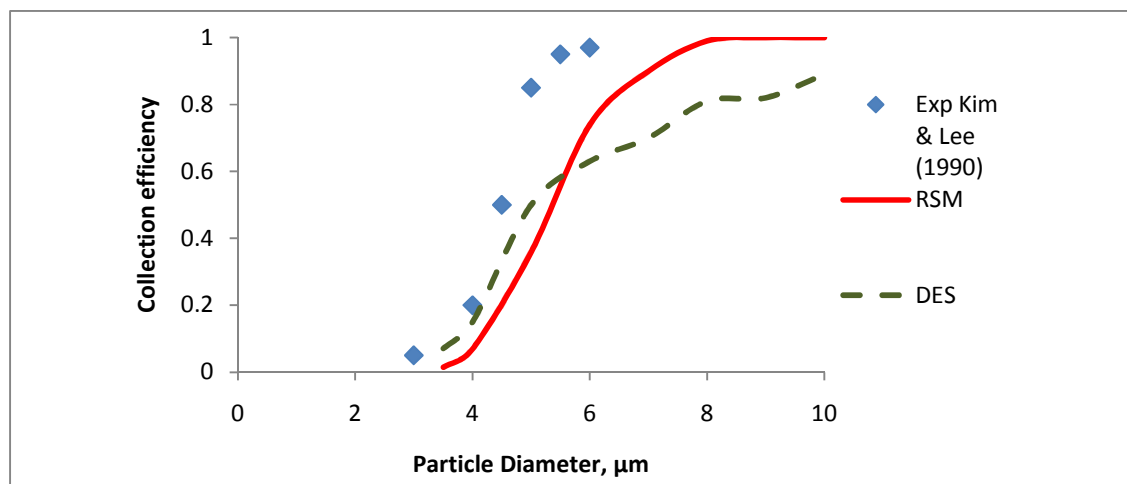


Figure 4.6: Simulated collection efficiencies for Kim & Lee cyclone II ( $P = 1$  atm,  $T = 273$  K,  $v_i = 18.4$  lpm,  $D_e = 1.36$  cm). Data point from Kim and Lee (1990).

Basically, the two cyclones show the same trend of collection efficiency. Both cyclones demonstrate that collection efficiency increase if either inlet velocity or particle size increase. Increasing inlet velocity increases the centrifugal force and therefore efficiency, but at the same time decreases the pressure drops. From Air Pollution Control Technology Handbook by Schnelle & Brown (2002), increasing gas flow rate through given cyclone will have effect on collection efficiency such as:

$$\frac{Pt_2}{Pt_1} = \left(\frac{Q_1}{Q_2}\right)^{0.5}$$

where  $P_t$  is penetration and  $Q$  is volumetric flow rate. Particle penetration is equal to  $1 - \eta$  (particle removal efficiency) and inlet velocity can be determined by dividing volumetric flow with inlet vane area (a.b).

The efficiency curve becomes sharper as inlet flow rate increases. Collection efficiency curve is seen sharper as the air flow rates increase, as shown on figure 4.1 – 4.6. Shape of collection efficiency curves for a fixed flow rate is seen to remain roughly the same regardless of cyclone body size and exit tube size. Separation of solids from the gas is due to classification in the vortex due to centrifugal forces. The centrifugal force field established by swirling flow inside the entire cyclone. When centrifugal force acts on a particle, it causes a radial settling velocity. This settling velocity is superimposed by an axial flow component. It is obvious that very coarse particles with high settling velocity will reach the wall and finer particles with a high settling velocity will reach the wall and finer particles may drag to inner vortex where they are classified according to cut size and efficiency grade curve. Main volumetric flow rate and the clarification area will determine whether a particle is separated at the wall or not.

From exit tube size prospect, it is observed that particle collection efficiency is found to decrease with increasing exit tube size. This observation can be seen in figure 4.7 where the larger  $D_e/D$  has lower collection efficiency. For most cyclone design application the ratio of the exit tube to cyclone body is kept roughly the same, so the change in particle size with quite big magnitude is not widely recognized. The influence of exit tube size toward collection efficiency is seen significant as it manipulates both inner and outer spiral flow patterns. If diameter of the exit tube is large, the flow pattern may not be sharp, so the particle may likely exit at the top outlet without reaching the bottom part of the cyclone. Small exit tube size will induce a well defined outer spiral flow and a small and long inner spiral flow forcing larger number of particles to travel via bottom part of the cyclone, thus increasing the chances of the particles to fall into bottom trap.



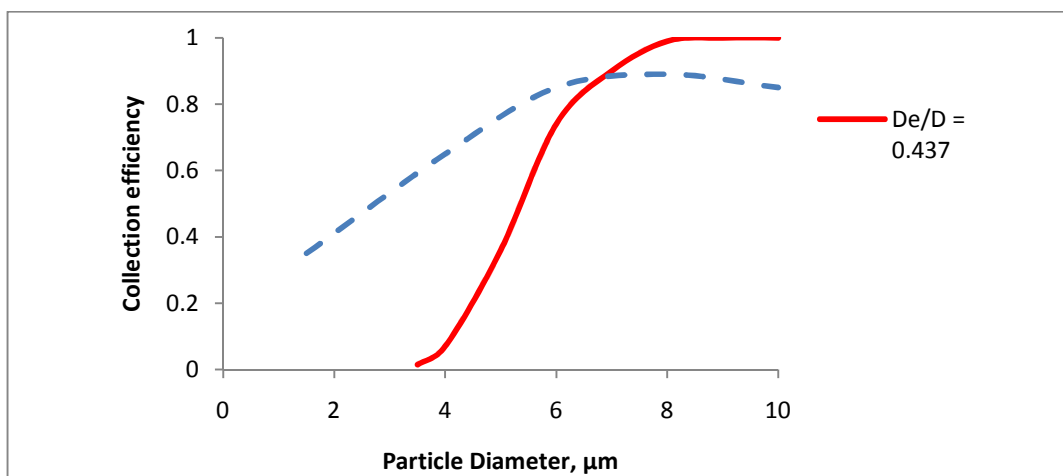


Figure 4.7: RSM prediction of collection efficiency for two different tube sizes, cyclone 1 & 2 for  $v_i = 18.4$  lpm.

Separation of particles in the cyclone is due to the centrifugal force caused by the spinning gas stream; this force throws particles outward to the cyclone wall. Opposing this outward particle motion is an inward drag force caused by gas flowing toward the axis of the cyclone prior to discharge. The centrifugal force developed inside the cyclone accelerates the settling rate of the particles, thereby separating them according to specific gravity in the medium. Denser particle is flung to the outer wall of the cyclone where the settling velocity is at its lowest and progresses downwards along the cyclone wall in a spiral flow pattern until it exits at the bottom cone. For smaller particles, the drag force maybe sufficient to move the particle towards the center of the cyclone. If the inward drag force is strong enough, and particles reach the central flow region where the flow is ascending, they will most likely escape together with the outgoing gas. However, the centrifugal force will increase, as the particle is moving towards the radius of the outlet pipe due to the increased tangential velocity. Thus the force on a particle may balance at some radius where the particle theoretically stops its radial movement and revolves in an orbit with constant radius. Shephred et al. (1939) wrote that particle can also change path due to secondary effects such as turbulence eddies or collision with other particles. At the bottom cone, a reverse vortex begins to form creating a low pressure zone flowing upwards along the axis of the cyclone, through vortex finder and exit at the overflow.

Kim & Lee (1990) added extra qualitative experiment to determine the location of particle deposited within the inner structure of a cyclone. They've found that large number of particles deposited in the lower part of the cyclone body. Particles that move to bottom region of the cyclone by the downward spiral flow may become deposited by centrifugal force. Sudden change in the flow direction in this region will would cause large particle to deviate from air stream lines and deposited onto the wall. Some particles entering the cyclone tangentially through the inlet tube become deposited on the cyclone wall by the impaction mechanism before fully turning around the annular gap between the exit tube and the inner wall of the cyclone body. Finally, Kim & Lee (1990) share the agreement that particle collection in cyclones occurs mainly by centrifugal force in the main cyclone body section. So any disturbance on centrifugal force will definitely reduce the collection efficiency of cyclone.

Both turbulence model predict the expected s-curve of cyclone collection efficiency, where RSM shown excellent agreement with Kim & Lee (1990) experimental data. Fraser (2003) describe that Reynolds Stress turbulence model yields an accurate prediction of swirl flow pattern, axial velocity, tangential velocity and pressure drop on cyclone simulations. The thoroughness of this model numerically solving as much as 7 equations, the performance is as expected. Besides, RSM has been favorite numerical approach among researchers since its introduction. Meanwhile, DES prediction did follow the 's' shape curve but not as precise and collection efficiency seldom reach 1 as it supposed when reaching particular particle diameter. DES inability is due to its incompatibility simulating the multiphase separation occurred inside the cyclone.

Concept of "saltation" by Kalen and Zenz indicates that, more than just diminishing return with increased velocity, collection efficiency actually decreases with excess velocity. At velocities greater than the saltation velocity, particles are not removed when they reach the cyclone wall, but are kept in suspension as the high velocity causes the fluid boundary layer to be very thin.

## 4.2 Cyclone Pressure Drop

Pressure drop across the cyclone is a great indicator of cyclone power usage. Pressure drops provide driving force that generates gas velocity and centrifugal force inside the cyclone. An accurate prediction of pressure drop will directly determine operating cost of a cyclone. In this study pressure drop of a cyclone is calculate as pressure difference between inlet pressure and top outlet pressure. Basically, many researchers found that cyclone pressure drop is directly proportional to inlet velocity. The Air Pollution Control Technology Handbook by Schnelle & Brown gives the correlation between pressure drop and inlet velocity of the cyclone as:

$$\Delta P = \frac{1}{2g_c} \rho_g V_i^2 N_H$$

where  $\Delta P$  = pressure drop

$\rho_g$  = gas density

$V_i$  = inlet gas velocity

$N_H$  = pressure drop expressed as number of the inlet velocity heads

The simulations of both RSM and DES models show the same agreement. Pressure drop of both cyclone I & II are both compared with Kim & Lee (1990) for two different inlet velocities as shown in table 4.1. It should be noted RSM prediction of both model shows excellent agreement with experimental data for both cyclones while DES prediction shown fair agreement with experimental with error less than 30%. This is due to incompatibilities of DES model in predicting multiphase (air & particle) condition of the cyclone.

| Cyclone-I Pressure Drop (Pa)  |           |           |              |
|-------------------------------|-----------|-----------|--------------|
| Inlet Velocities              | RSM Model | DES Model | Experimental |
| 12.4                          | 31.236    | 37.65     | 27.4         |
| 18.4                          | 69.32     | 72.33     | 60.279       |
| Cyclone-II Pressure Drop (Pa) |           |           |              |
| Inlet Velocities              | RSM Model | DES Model | Experimental |
| 12.4                          | 16.44     | 21.4      | 13.7         |
| 18.4                          | 52.7      | 49.8      | 43.59        |

Table 4.1: Fluent predictions for cyclone I & II pressure drop. Experimental data obtained from Kim and Lee (1990).

The pressure drop was found to decrease with increase on exit tube diameter. If exit tube size is enlarged until it reaches the diameter of cyclone body, the pressure drop will increase again. Kim and Lee (1990), describe that the reduces in pressure drop when the exit diameter become larger happens due to significant portion of pressure drops occur inside the exit tube. When the exit tube diameter too large, the sudden increase of pressure drop indicates that energy loss occurs in the annular gap between exit tube and cyclone wall.

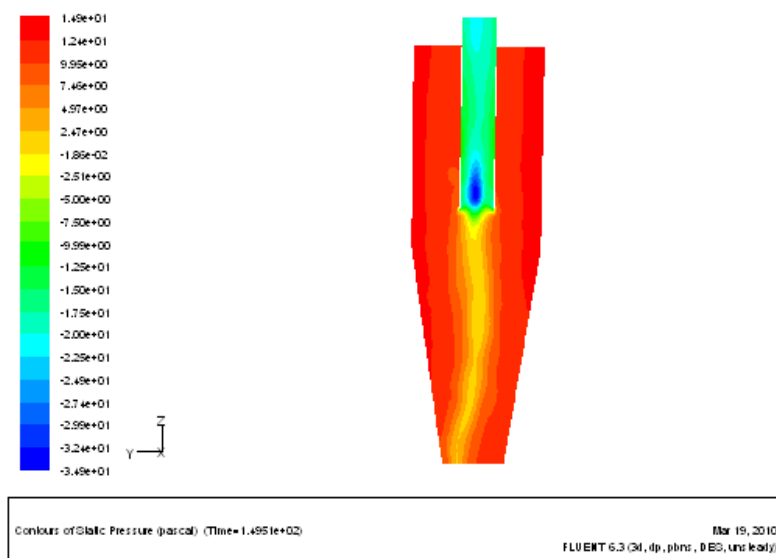


Figure 4.8: Pressure profile of cyclone as simulated by FLUENT. The dark blue region indicates the lowest pressure while dark red region indicate the highest pressure inside the cyclone.

Generally, two factors that induce pressure drops across the cyclone are the wall friction and the contraction of the inner vortex on entering the vortex finder. Two parts in the cyclone contribute the total pressure drops across the cyclone. The first part is pressure lost in the separation zone, caused by the friction between gas and solid surface. Separation zone pressure loss contributes about 80% of total pressure drop, depending on tangential velocity, the radius and the mean axial velocity, the surface area, and wall friction. Another 20% of pressure drops is contributed by pressure loss occurs in vortex finder or exit tube section, which being manipulated in this study. The pressure loss of vortex finder can be determined by relationship between tangential velocity, the radius and the mean axial velocity in exit tube of a cyclone.

The intention of optimizing cyclone performance can be achieved by maximizing the collection efficiency and reducing pressure drop across the cyclone. Unfortunately, this two measure usually conflicting with each other, where efforts in increasing collection efficiency will result in unwanted incremental pressure drop.

### **4.3 Particle 50% Cut-Off Size**

Several methods for estimating cyclone efficiency have been developed. Most of these methods utilize a particle size term called a 50 % particle cut size. 50 % particle cut size can be defined as particle diameter taken when collection efficiency equals to 50%. The  $d_{50}$  cut size corresponds to a size where 50% of particles smaller then  $d_{50}$  and 50% of particles larger then  $d_{50}$  will be collected. 50 % particle cut size is usually utilized in order to compare an increased number of the data sets with theories in systematic ways. As in this study, the effect of exit tube diameter can be studied using  $d_{50}$ . Table 4.2 shows the comparison between 50% cut-off diameter between CFD prediction and experimental data by Kim & Lee (1990).

| <b>Cyclone-I 50% Cut-Off Diameter</b>  |                  |                  |                     |
|--|------------------|------------------|---------------------|
| <b>Inlet Velocities</b>                | <b>RSM Model</b> | <b>DES Model</b> | <b>Experimental</b> |
| 8.8                                    | 5.97             | 6.5              | 6.1                 |
| 12.4                                   | 4.5              | 5.4              | 4.2                 |
| 18.4                                   | 2.4              | 4.0              | 1.806               |
| <b>Cyclone-II 50% Cut-Off Diameter</b> |                  |                  |                     |
| <b>Inlet Velocities</b>                | <b>RSM Model</b> | <b>DES Model</b> | <b>Experimental</b> |
| 8.8                                    | 6.8              | 5.9              | 6.6                 |
| 12.4                                   | 5.3              | 5.3              | 5                   |
| 18.4                                   | 5                | 4.8              | 4.5                 |

Table 4.2: Fluent predictions for cyclone 50% cut-off diameter. Experimental data obtained from Kim and Lee (1990)

Both model RSM and DES prediction shows excellent agreement with experimental data, even though DES still lacking in precision compared to RSM due to its incompatibilities. The cut 50% cut off diameter decreases when velocity increases, and at the same time demonstrate that  $d_{50}$  increases with increases exit diameter. The latter observation supports that efficiency curve become stiffer with increasing inlet velocity. Somehow, if the flow rate is fixed, efficiency curve cease to change even with change in exit diameter. So it is possible to alter the diameter particle without deteriorating sharpness just by simply adjusting the exit tube diameter.

## CHAPTER 5

### CONCLUSION & RECOMMENDATION

#### 5.0 Conclusion

The CFD code predicts very well the collection efficiency, pressure drop and cut-off size of Kim & Lee experimental miniature cyclone. Two turbulence models were used in this study, the RSM and DES. The RSM model was found to be much closer to experimental data compared to DES model. DES liability was due to its incompatibilities in simulating multiphase condition of cyclone separation, in this case between gas (air) and solids (DOP particles). Simulation data revealed that increases inlet velocity will make efficiency curve stiffer, or the  $d_{50}$  become smaller. With respect to exit tube size, particle collection efficiency is found to increase when exit tube size become smaller. It is believed that the exit tube size largely influencing the flow field inside the cyclone, including the pattern of the outer and the inner spiral flows. Pressure drops simulation shown that the pressure drop across the cyclone to be dependent on cyclone flowrate. As exit tube increases, the pressure drop was found to be decreased. Also, when exit tube size increased until as large as cyclone body, the pressure drops increase again. Cut-off diameter was simulated to clearly shows the relationship between  $d_{50}$  and the cyclone exit tube size diameter which directly proportional.

## 5.1 Future Work

There are many more parameter that can affect the performance of cyclone such as high operating temperature and pressure, dust loading, and cyclone body diameters. Every single parameter can be simulated using CFD. Latest Fluent code for DES model should be use for next studies to improve its prediction, where perhaps the incompatibility on predicting multiphase condition has been overcome. There are many empirical model created from experimental data that can successfully predict the cyclone collection efficiency and pressure drop. For example the Barth and Leith-Licht theories which able to predict efficiencies correctly. The data calculated then is compare with experimental data and simulation data to verify theories accuracy.



**REFERENCES:**

*Bohnet, M. (1995) "Influence of Gas Temperature on Separation Efficiency of Aerocyclones", Chemical Engineering and Processing 34 (1995) 151-156*

Chen, C. C., Lai, C. Y., Shih, T. S., & Yeh, W. Y. (1998). Development of respirable aerosol samplers using porous foams. *American Industrial Hygiene Association*, 59, 766–773.

*Chen, J. and Shi, M. (2005), "Analysis on Cyclone Collection Efficiencies at High Temperature", CHINA PARTICUOLOGY Vol. 1, No. 1, 20-26, 2003*

T. G. Chuah, Jolius Gimbun, Thomas S. Y. Choong, and A. Fakhru'l-Razi (2003). "Numerical Prediction of Pressure Drops". *Journal of Chemical Engineering and Environment*, Vol. 2, No. 2, pp. 67-71, 2003

D. Leith, W. Licht, The collection efficiency of cyclone type particle collectors: a new theoretical approach, *AIChE Symposium Series 68 (1972) 196–206*.

Iozi, D. L. and Leith, D. (1989) Effect of cyclone dimensions on gas flow pattern and collection efficiency. *Aerosol Sci. Technol.* 10, 491-500.

J. Gimbun, T.G. Chuah, A. Fakhru'l-Razi, Thomas S.Y. Choong, The influence of temperature and inlet velocity on cyclone pressure drop: a CFD study, *Chemical Engineering and Processing* 44 (1) (2005) 7 – 12.

Kim, J. C. and Lee, K. W. (1990) Experimental Study of Particle Collection by Small Cyclones. *Aerosol Sci. Technol.* 12, 100331015.

Lapple, C. E. (1950) Gravity and centrifugal separation. *Ind. Hyg. Q.* 11, 40

Moore, M. E., & McFarland, A. R. (1990). Design of Stairmand-type sampling cyclones. *American Industrial Hygiene Association*, 51, 151–159.

Petty, C.A., Parks, S.M., Shao, S.M., 2000. The use of small hydrocyclones for downhole separation of oil and water. Svarovsky, L., Thew, M. (Eds.), 5th International Conference on Cyclone Technologies. BHR Group Limited, The Fluid Engineering Centre, Cranfield, Bedfordshire

Smith, W. B., Cushing, K. M., & Wilson, R. R. (1982). Cyclone sampling for measuring the concentration of inhalable particles in process streams. *Journal of Aerosol Science*, 13, 259–267.

Saltzman, B. E., & Hochstrasser, J. M. (1983). Design and performance of miniature cyclone for respirable aerosol sampling. *Environmental Science and Technology*, 17, 418–424.

T. Fraser, Personal Communication, fraserta1@cf.ac.uk, www.cfd-online.com, 2003.

Saltzman, B. (1984) Generalised performance characteristics of miniature cyclones for atmospheric particulate sampling. *Am. Ind. Hyg. Assoc. J.* 45, 671-680.

T.G. Chuah, J. Gimbun, Thomas S.Y. Choong, A CFD study of the effect of cone dimensions on sampling aerocyclones performance and hydrodynamics, *Powder Technology* 162 (2006) 126 – 132.

Tsai, C. J., Chein, H. M., Chang, S. T., & Kuo, J. Y. (1996). Performance evaluation of an API aerosizer. '96 International Conference on Aerosol Science and Technology, Taipei, Taiwan (pp. 559–568).

*Silva, P. D., Briens, C., Bernis, A., (2003) Powder Technol. 131, 111*

Shepherd, G. B. and Lapple, C. E. (1939) Flow pattern and pressure drop in cyclone dust collectors. *Ind. Eng Chem.* 31, 972.

W. Barth, Berechnung und Auslegung von Zyklonabscheidern aufgrund neuerer Untersuchungen, *Brennstoff, Wa'rme, Kraft* 8 (1956) 1– 9.

W.D. Griffiths, F. Boysan, Computational fluid dynamics (CFD) and empirical modelling of the performance of a number of cyclone samplers, *Journal of Aerosol Science* 27 (1996) 281–304.

Wu, J. J., Copper, D. W., & Miller, R. J. (1989). Virtual impactor aerosol concentrator clean room monitoring. *Journal of the Environmental Science*, 32, 52–56.

Zhu, Y., & Lee, K. W. (2001). Experimental study on small cyclones operating at high flow rates. *Journal of Aerosol Science*, 30, 1303–1325.

## APPENDIX

### Appendix A Collection Efficiency Data of Cyclone 1

*Table A1: Inlet Velocity = 8.8 lpm*

| Experimental Data<br>(Kim and Lee, 1990)       |                          | Reynold Stress Model (RSM)<br>Prediction       |                          | Detached Eddy Simulation<br>(DES) Prediction   |                          |
|--|--------------------------|--|--------------------------|--|--------------------------|
| Diameter<br>particle, Dp,<br>( $\mu\text{m}$ ) | Collection<br>Efficiency | Diameter<br>particle, Dp,<br>( $\mu\text{m}$ ) | Collection<br>Efficiency | Diameter<br>particle, Dp,<br>( $\mu\text{m}$ ) | Collection<br>Efficiency |
| 3.3543   | 0.0106                   | 3.5088   | 0.0393                   | 3.9912   | 0.0706                   |
| 3.8542   | 0.1239                   | 3.9693   | 0.1481                   | 4.9342   | 0.1379                   |
| 4.7129   | 0.2123                   | 4.5395   | 0.2522                   | 5.636  | 0.3102                   |
| 5.4279   | 0.3449                   | 5.3947   | 0.3743                   | 6.2281   | 0.4052                   |
| 5.9773   | 0.489                    | 6.0746   | 0.4692                   | 6.9737   | 0.4454                   |
| 6.8082   | 0.7464                   | 7.0614   | 0.6412                   | 8.3772   | 0.5485                   |
| 8.2314   | 0.8866                   | 8.4211   | 0.7717                   | 9.1667   | 0.6661                   |
| 9.801  | 0.9654                   | 9.1667   | 0.7937                   | 9.8246   | 0.7291                   |

*Table A2: Inlet Velocity = 12.4 lpm*

| Experimental Data<br>(Kim and Lee, 1990)       |                          | Reynold Stress Model (RSM)<br>Prediction       |                          | Detached Eddy Simulation<br>(DES) Prediction   |                          |
|--|--------------------------|--|--------------------------|--|--------------------------|
| Diameter<br>particle, Dp,<br>( $\mu\text{m}$ ) | Collection<br>Efficiency | Diameter<br>particle, Dp,<br>( $\mu\text{m}$ ) | Collection<br>Efficiency | Diameter<br>particle, Dp,<br>( $\mu\text{m}$ ) | Collection<br>Efficiency |
| 1.6704   | 0.0353                   | 3.5088   | 0.0393                   | 4.005  | 0.2751                   |
| 3.3071   | 0.238                    | 3.9693   | 0.1481                   | 5.0159   | 0.3663                   |
| 3.8244   | 0.4274                   | 4.5395   | 0.2522                   | 5.9916   | 0.5421                   |
| 4.6183   | 0.6947                   | 5.3947   | 0.3743                   | 6.3588   | 0.5522                   |
| 5.4109   | 0.8942                   | 6.0746   | 0.4692                   | 7.0016   | 0.586                    |
| 5.9621   | 0.9347                   | 7.0614   | 0.6412                   | 8.5268   | 0.7109                   |
| 6.825  | 0.965                    | 8.4211   | 0.7717                   | 10.0143  | 0.7783                   |
| 8.2381   | 0.9749                   | 9.9561   | 0.7745                   |  |                          |

*Table A3: Inlet Velocity = 18.4 lpm*

| Experimental Data<br>(Kim and Lee, 1990)       |                          | Reynold Stress Model (RSM)<br>Prediction       |                          | Detached Eddy Simulation<br>(DES) Prediction   |                          |
|--|--------------------------|--|--------------------------|--|--------------------------|
| Diameter<br>particle, Dp,<br>( $\mu\text{m}$ ) | Collection<br>Efficiency | Diameter<br>particle, Dp,<br>( $\mu\text{m}$ ) | Collection<br>Efficiency | Diameter<br>particle, Dp,<br>( $\mu\text{m}$ ) | Collection<br>Efficiency |
| 1.0993   | 0.4318                   | 1.4706   | 0.3537                   | 2.9945   | 0.2532                   |
| 1.7904   | 0.6423                   | 2.0116   | 0.4668                   | 3.5788   | 0.3743                   |
| 3.1535   | 0.9372                   | 3.3566   | 0.5947                   | 4.2505   | 0.479                    |
| 3.7398   | 0.9687                   | 3.8988   | 0.6548                   | 4.7494   | 0.5269                   |
| 4.6305   | 0.9956                   | 4.8966   | 0.7548                   | 6.8976   | 0.7104                   |
| 6.7611   | 0.9917                   | 6.8507   | 0.8693                   | 8.6113   | 0.8783                   |

## Collection Efficiency Data of Cyclone II

Table A4: Inlet Velocity = 8.8 lpm

| Experimental Data<br>(Kim and Lee, 1990)       |                          | Reynold Stress Model (RSM)<br>Prediction       |                          | Detached Eddy Simulation<br>(DES) Prediction   |                          |
|--|--------------------------|--|--------------------------|--|--------------------------|
| Diameter<br>particle, Dp,<br>( $\mu\text{m}$ ) | Collection<br>Efficiency | Diameter<br>particle, Dp,<br>( $\mu\text{m}$ ) | Collection<br>Efficiency | Diameter<br>particle, Dp,<br>( $\mu\text{m}$ ) | Collection<br>Efficiency |
| 3  | 0.05                     | 4  | 0.07                     | 3.5  | 0.07                     |
| 4  | 0.2                      | 5  | 0.36                     | 4  | 0.15                     |
| 4.5  | 0.5                      | 6  | 0.74                     | 5  | 0.5                      |
| 5  | 0.85                     | 7  | 0.9                      | 6  | 0.63                     |
| 5.5  | 0.95                     | 8  | 0.99                     | 7  | 0.7                      |
| 6  | 0.97                     | 9  | 1                        | 8  | 0.81                     |

Table A5: Inlet Velocity = 12.4 lpm

| Experimental Data<br>(Kim and Lee, 1990)       |                          | Reynold Stress Model (RSM)<br>Prediction       |                          | Detached Eddy Simulation<br>(DES) Prediction   |                          |
|--|--------------------------|--|--------------------------|--|--------------------------|
| Diameter<br>particle, Dp,<br>( $\mu\text{m}$ ) | Collection<br>Efficiency | Diameter<br>particle, Dp,<br>( $\mu\text{m}$ ) | Collection<br>Efficiency | Diameter<br>particle, Dp,<br>( $\mu\text{m}$ ) | Collection<br>Efficiency |
| 3.5  | 1.00E-01                 | 3.5  | 0                        | 3.5  | 0.05                     |
| 5  | 0.4                      | 4  | 0.1                      | 4  | 0.18                     |
| 6  | 0.64                     | 5  | 0.3                      | 5  | 0.36                     |
| 7  | 0.8                      | 6  | 0.55                     | 6  | 0.5                      |
| 8  | 0.89                     | 7  | 0.69                     | 7  | 0.62                     |
| 9  | 0.98                     | 8  | 0.8                      | 8  | 0.72                     |
| 10   | 1                        | 9  | 0.85                     | 9  | 0.78                     |

*Table A6: Inlet Velocity = 18.4 lpm*

| Experimental Data<br>(Kim and Lee, 1990)       |                          | Reynold Stress Model (RSM)<br>Prediction       |                          | Detached Eddy Simulation<br>(DES) Prediction   |                          |
|--|--------------------------|--|--------------------------|--|--------------------------|
| Diameter<br>particle, Dp,<br>( $\mu\text{m}$ ) | Collection<br>Efficiency | Diameter<br>particle, Dp,<br>( $\mu\text{m}$ ) | Collection<br>Efficiency | Diameter<br>particle, Dp,<br>( $\mu\text{m}$ ) | Collection<br>Efficiency |
| 4  | 0.00E+00                 | 4.8  | 0                        | 4.5  | 0.05                     |
| 5  | 0.06                     | 5  | 0.05                     | 5  | 0.2                      |
| 6  | 0.24                     | 6  | 0.25                     | 6  | 0.4                      |
| 7  | 0.51                     | 7  | 0.4                      | 7  | 0.52                     |
| 8  | 0.73                     | 8  | 0.55                     | 9  | 0.6                      |
| 9  | 0.82                     | 9  | 0.65                     | 10   | 0.65                     |
| 4  | 0.00E+00                 | 4.8  | 0                        | 4.5  | 0.05                     |

\*Pressure Drops and Cut-off diameter data are similar as in section 4.2 and 4.3

# MODELLING OF HIGH EFFICIENCY MINIATURE AEROCYCLONE

**Aiman Hakim Bin Badarisman**

*Faculty of Chemical and Natural Resources Engineering,  
Universiti Malaysia Pahang, Lebuhraya Tun Razak,  
26300 Gambang, Pahang, Malaysia.  
E-mail : aimanhkim@gmail.com*

## Abstract

Cyclone separation is one of the largely recognized methods of removing particulate in air, gas or water stream without help from filters. Cyclone is favorite separation device in various industries due to its simplicity, inexpensive design and minimum operational cost. In this research, the objective is to maximizing the performance of miniature aerocyclone. The performance of aerocyclone can be analyzed by its collection efficiency and pressure drop. In past studies, expensive and time consuming experiment were conducted in order to analyze the performance of cyclone, but Computational Fluid Dynamics (CFD) software that being implemented in this research has successfully solve the problem. FLUENT is a commercially available CFD code that utilizes the finite volume formulation to carry out coupled or segregated calculations. For the turbulent flow in a cyclone the key to the success of CFD lies with the accurate description of the turbulent behavior of the flow. The simulation starts with meshing of miniature cyclone via Gambit software. The meshed cyclone was then transferred into FLUENT software for simulation, where all the boundary condition is programmed in the software. After simulation was completed, the data was then extracted and converted in the function of cyclone collection efficiency and pressure drop. The results show the influence of inlet velocity and exit tube size on cyclone performance and significant conclusion were made. The performances of turbulence model used in the simulation were then compared.

Keywords: Cyclone; CFD; Inlet Velocity; exit tube size; pressure drops; collection efficiency

## 1. INTRODUCTION

Cyclone separation is one of the largely recognized methods of removing particulate in air, gas or water stream without help from filter. These particulates are removed through spinning, often turbulent, flow of fluid plus a little help from gravity. The device is called a cyclone. A conventional cyclone looks like a cylindrical or conical where high velocity air rotating within it. At the top of the cyclone (wide end) air flow as vortex and end up at the narrow end or the bottom of the cyclone. The air flow then goes out through top in a straight stream via center of the cyclone, meanwhile denser particle in the rotating stream have too much inertia to follow the tight curve of the stream and strike the outside wall, falling then to the bottom of the cyclone where they can be removed. Within the conical section of the cyclone the rotational radius of stream is reduced whenever the flow move nearer to the narrow bottom end, thus separating smaller and smaller particles. The outlet flow at the top end often labeled as major flow meanwhile the outlet flow at bottom where dust container is placed often labeled as minor flow.

When engineers want to design a cyclone, there are two important parameters that need to be considered. These parameters are collection efficiency of particle and pressure drop across the cyclone. An accurate prediction of cyclone pressure drop is very important because it relates directly to operating costs. Higher inlet velocities give higher collection efficiencies for a given cyclone, but this also increases the pressure drop across the cyclone (Gimbun et al. 2004). Particle size distribution is also strongly influence the collection efficiency. Cyclone collection efficiencies can reach 99% for particles bigger than 5  $\mu\text{m}$  (Silva et al. 2003). Their simple design, low maintenance costs, and adaptability to a wide range of operating conditions such as sizes and flow rates make cyclones one of the most widely used particle removal devices. By using suitable materials and methods of construction, cyclones may be adapted for use in extreme operating conditions: high temperature, high pressure, and corrosive gases (Gimbun et al. 2004).

CFD is an acronym for Computational Fluid Dynamics, or the art of using a computer to predict how gases and liquids flow. CFD has a great potential to predict the flow field characteristics and particle



trajectories inside the cyclone as well as the pressure drop (Griffith & Boysan, 1996). The numerical techniques and turbulence models that employed in CFD is capable to solve the complicated swirling turbulence flow in cyclone.

## 1.1 CFD Approach

Cyclone simulation began in 1982, with pioneering work of Boysan et al. which used an axis symmetry model and a hybrid model of turbulence composed of a combination of the k-s model and the algebraic stress model. After that, Pericleous (1987) presented a new axis-symmetry model with turbulence prediction which included the simplification of Prandtl's mixture length theory to simulate hydrocyclones. Duggins and Frith (1987) presented the failures of the k-ε model in simulating swirling flows and proposed a new turbulence model using a combination of the k-s model and the mixture length model to introduce the anisotropic behavior of the Reynolds stress. Madsen et al. (1994), using a version of the algebraic stress model of turbulence, presented a new simulation of cyclones solving the gas phase by the Flow-3D computational code e developing the Lagrangian model for the particles. Meier and Mori (1996), presented a new model of turbulence of the gas phase considering the anisotropic behavior of the Reynolds stress by using a combination between the k-ε model and the mixture length theory of Prandtl. The results were validated by four test cases from the literature and proved to be satisfactory.

This study represents the prediction of miniature aero-cyclone collection efficiency, pressure drops and 50% particle cut-off diameter using CFD simulation. At the same time, the influence of exit tube dimension, turbulence models and inlet velocity toward these three parameters will be concluded based on the CFD prediction. Finally these prediction data will be verified with experimental data from Kim and Lee experimental studies.

## MODELLING APPROACH

### 2.1 Governing Equation for Fluid Flow inside a Cyclone

Fluid flows have long been mathematically described by a set of nonlinear, partial differential equations, namely the Navier-Stokes equations, but, except in a few simple situations, theoretical solutions to the Navier-Stokes equations are still very difficult to find. Even with the advent of the modern digital computers, direct numerical solutions to the Navier-Stokes equations for the fluid flow of engineering interest is still not easy. A practical way of simulating fluid flows in engineering applications is to use turbulence models and solve for the mean fluid velocity and pressure. It is important to note that most fluid flows in cyclones operate in the turbulent fluid flow regime, whilst some small cyclones may well be operated in the transition flow regime where fluid flow structures are different from those which exist in a fully developed turbulent flow and therefore different procedures may be employed for the modelling of the transition flow. However, the problem has been limited to a discussion of fully developed turbulent fluid flows in cyclones. For the steady and incompressible fluid flow in cyclones, the following Reynolds-averaged Navier-Stokes equations are employed:

#### Navier-Stokes Equation

$$\rho u^j \frac{\partial u^i}{\partial x^j} = - \frac{\partial p}{\partial x^i} + \frac{\partial}{\partial x^j} \left[ \mu \left( \frac{\partial u^i}{\partial x^j} + \frac{\partial u^j}{\partial x^i} \right) \right] + \frac{\partial \tau^{ij}}{\partial x^j} \quad (1)$$

#### Continuity Equation

$$\frac{\partial u^i}{\partial x^i} = 0 \quad (2)$$

where the superscripts  $i, j = 1, 2, 3$  indicate the components in the Cartesian co-ordinate system,  $u^i, p, \rho$  and  $\mu$  are the fluid velocity, pressure, density and molecular viscosity, respectively, and

$$\tau^{ij} = -\overline{\rho u^i u^j} \quad (3)$$

is known as the Reynolds stress tensor which represents the effects of the turbulent fluctuations on the fluid flow. The overbar represents a Reynolds average and the dash represents the fluctuating part. For convenience, the overbars on top of the mean fluid velocity  $u^i$  and the pressure  $p$  have been removed in

equations (1) and (2) and in the remainder of this paper. However, the Reynolds-averaged Navier-Stokes equations (1) and (2) are not closed unless a model is provided which ties the Reynolds stress tensor  $\tau^{ij}$  to the global history of the mean fluid velocity  $ui$  in a physically consistent fashion.

## 2.2 Turbulence modelling

Reynolds Stress models (RSM) solve for individual Reynolds stresses and for the turbulent dissipation  $\varepsilon$ . The Reynolds Stress model assumes that the factors within it contain no dependence on the Reynolds number of the flow. However it should be noted that this is not always true especially at moderate Reynolds numbers. The central concept of the Reynolds stress model is that the stress tensor  $R_{ij}$  is determined locally within the cell. The Reynolds Stress turbulence model yields an accurate prediction of swirl flow pattern, axial velocity, tangential velocity and pressure drop on cyclone simulations (Reddy, 2003; Fraser, 2003; Fredriksson, 1999).

The Reynolds stress model involves calculation of the individual Reynolds stresses,  $\overline{\rho u^i u^j}$ , using differential transport equations. The individual Reynolds stresses are then used to obtain closure of the Reynolds-averaged momentum equation. The exact transport equations for the transport of the Reynolds stresses  $\overline{u_i' u_j'}$  may be written as follows:

$$\underbrace{\frac{\partial}{\partial t} (\overline{\rho u_i' u_j'})}_{\text{Time derivative}} + \underbrace{\frac{\partial}{\partial x_k} (\overline{\rho u_k u_i' u_j'})}_{C_{ij}=\text{Convection}} = - \underbrace{\frac{\partial}{\partial x_k} [\overline{\rho u_i' u_j' u_k'} + p(\overline{\delta_{ij} u_k'} + \overline{\delta_{ik} u_j'})]}_{D_{T,ij}=\text{Turbulent diffusion}}$$

$$- \underbrace{\rho \left( \overline{u_i' u_k'} \frac{\partial u_j}{\partial x_k} + \overline{u_j' u_k'} \frac{\partial u_i}{\partial x_k} \right)}_{P_{ij}=\text{Stress production}} + \underbrace{\frac{p}{\rho} \left( \frac{\partial u_i'}{\partial x_j} + \frac{\partial u_j'}{\partial x_i} \right)}_{\phi_{ij}=\text{Pressure strain}} - \underbrace{2\mu \frac{\partial u_i'}{\partial x_k} \frac{\partial u_i'}{\partial x_k}}_{\varepsilon_{ij}=\text{Dissipation}}$$

$$- \underbrace{2\rho \Omega_k \left( \overline{u_j' u_m'} \varepsilon_{ikm} + \overline{u_i' u_m'} \varepsilon_{jkm} \right)}_{F_{ij}=\text{Production by system rotation}}$$

The  $\Omega_k$  is an angular velocity and both  $\varepsilon_{ikm}$  and  $\varepsilon_{jkm}$  are permutation tensors. Of the various terms in these exact equations,  $C_{ij}$ ,  $D_{L,ij}$ ,  $P_{ij}$ , and  $F_{ij}$  do not require any modelling. However,  $D_{T,ij}$ ,  $\phi_{ij}$ , and  $\varepsilon_{ij}$  need to be modelled to close the equations. The reason is simply because the averaging procedure of  $\overline{u_i' u_j' u_k'}$  will generate a lot of unknown variables and it becomes impossible to solve them directly.

The turbulent diffusivity transport term is modelled using a simplified form of the generalised gradient diffusion hypothesis as:

$$D_{T,ij} = \frac{\partial}{\partial x_k} \left[ \frac{\mu_t}{\sigma_k} \frac{\partial (\overline{u_i' u_j'})}{\partial x_k} \right]$$

where  $P = 0.5P_{ij}$  is the turbulence production due to shear, and the constants are  $C_1 = 1.8$  and  $C_2 = 0.6$ .

The pressure strain term is modelled as:

$$\phi_{ij} = \frac{p}{\rho} \left( \frac{\partial u_i'}{\partial x_j} + \frac{\partial u_j'}{\partial x_i} \right) = -C_1 \frac{\varepsilon}{k} \left[ \overline{u_i' u_j'} - \frac{2}{3} \delta_{ij} k \right] - C_2 \left[ P_{ij} - \frac{2}{3} \delta_{ij} P \right]$$

The dissipation term is assumed to be isotropic and is approximated by:

$$\varepsilon_{ij} = 2\mu \frac{\partial u_i'}{\partial x_k} \frac{\partial u_i'}{\partial x_k} = \frac{2}{3} \delta_{ij} \varepsilon$$

The scalar dissipation rate is computed with a model transport equation similar to the one in the standard  $k-\varepsilon$  model.

The difficulties associated with the use of the standard LES models, particularly in near-wall regions, has led to the development of hybrid models that attempt

to combine the best aspects of RANS and LES methodologies in a single solution strategy. An example of a hybrid technique is the DES (Spalart et al., 1997) approach. This model attempts to treat near-wall regions in a RANS-like manner, and treat the rest of the flow in an LES-like manner. The model was originally formulated by replacing the distance function  $d$  in the Spalart-Allmaras (S-A) model with a modified distance function.

The SA one-equation model solves a single partial differential equation for a variable  $\tilde{\nu}$  which is related to the turbulent viscosity. The variable  $\tilde{\nu}$  is identical to the turbulent kinematic viscosity except in the near-wall (viscous-affected) region. The model includes a wall destruction term that reduces the turbulent viscosity in the log layer and laminar sub-layer. The transport equation for DES is:

$$\frac{\partial}{\partial t}(\rho\tilde{\nu}) + \frac{\partial}{\partial x_i}(\rho\tilde{\nu}u_i) = G_\nu + \frac{1}{\sigma_\nu} \left[ \frac{\partial}{\partial x_j} \left\{ (\mu + \rho\tilde{\nu}) \frac{\partial \tilde{\nu}}{\partial x_j} \right\} + C_{b2}\rho \left( \frac{\partial \tilde{\nu}}{\partial x_j} \right)^2 \right] - Y_\nu$$

The turbulent viscosity is determined via:

$$\mu_t = \rho\tilde{\nu}f_{v1}, \quad f_{v1} = \frac{\chi^3}{\chi^3 + C_{v1}^3}, \quad \chi \equiv \frac{\tilde{\nu}}{\nu}$$

where  $\nu = \mu / \rho$  is the molecular kinematic viscosity. The production term,  $G_\nu$ , is modelled as:

$$G_\nu = C_{b1}\rho\tilde{S}\tilde{\nu}, \quad \tilde{S} \equiv S + \frac{\tilde{\nu}}{k^2d^2}f_{v2}, \quad f_{v2} = 1 - \frac{\chi}{1 + \chi f_{v1}}$$

$S$  is a scalar measure of the deformation rate tensor which is based on the vorticity magnitude in the SA model. The destruction term is modelled as:

$$Y_\nu = C_{w1}\rho f_w \left( \frac{\tilde{\nu}}{d} \right)^2, \quad f_w = g \left[ \frac{1 + C_{w3}^6}{g^6 + C_{w3}^6} \right]^{1/6}, \quad g = r + C_{w2}(r^6 - r)$$

The closure coefficients for SA model are:

$$C_{b1} = 0.1355, \quad C_{b2} = 0.622, \quad \sigma_\nu = \frac{2}{3}, \quad C_{v1} = 7.1,$$

$$C_{w1} = \frac{C_{b1}}{k^2} + \frac{(1 + C_{b2})}{\sigma_\nu}, \quad C_{w2} = 0.3, \quad C_{w3} = 2.0, \quad k = 0.4187.$$

In the SA model the destruction term (eq. 4) is proportional to  $(\tilde{\nu}/d)^2$ . When this term is balanced with the production term, the eddy viscosity becomes proportional to  $\tilde{S}d^2$ . The Smagorinsky LES model varies its sub-grid-scale (SGS) turbulent viscosity with the local strain rate, and the grid spacing is described by  $\nu_{SGS} \propto \tilde{S}\Delta^2$  where  $\Delta = \max(\Delta x, \Delta y, \Delta z)$ . If  $d$  is replaced with  $\Delta$  in the wall destruction term, the SA model will act like a LES model. To exhibit both RANS and LES behaviour,  $d$  in the SA model is replaced by:

$$\tilde{d} = \min(d, C_{des}\Delta)$$

where  $C_{des}$  is a constant with a value of 0.65. Then the distance to the closest wall  $d$  in the SA model is replaced with the new length scale  $\tilde{d}$  to obtain the DES. The purpose of using this new length is that in boundary layers where  $\Delta$  far exceeds  $d$ , then the standard SA model applies since  $\tilde{d} = d$ . Away from walls where  $\tilde{d} = C_{des}\Delta$ , the model turns into a simple one equation SGS model, close to Smagorinsky's in the sense that both make the mixing length proportional to  $\Delta$ . The Smagorinsky model is the standard eddy viscosity model for LES. On the other hand, this approach retains the full sensitivity of RANS model predictions in the boundary layer. This model has never been applied to predict the stirred tank flows in the past and so this is an objective of the current study.

The finite volume method has been used to discretize the partial differential equations of the model using the SIMPLE method for pressure-velocity coupling and the Second Order Upwind scheme to interpolate the variables on the surface of the control volume. The segregated solution algorithm

was selected. The Reynolds stress (RSM) turbulence model was used in this model due to the anisotropic nature of the turbulence in cyclones. Standard Fluent wall functions were applied and high order discretization schemes were also used. The simulation is then solved with a coupling of unsteady and steady state solvers in FLUENT. To calculate the trajectories of particles in the flow, the discrete phase model (DPM) was used to track individual particles through the continuum fluid.

### 2.3 Cyclone dimension and modelling strategy

CFD simulation can only be operated with completely meshed miniature cyclone design. The cyclone simulated in this study is based on Kim and Lee (1990) miniature cyclone specification. Two cyclones were used in this study which only differs on the exit tube diameters, so the effect of vortex finder dimension can be analyze. Three different flow rates is chosen by Kim and Lee (1990) in their experiment, which are 8.8, 12.4 and 18.4 liter/min. These flow rates are also utilized in this simulation in order to observe influence of inlet velocity toward cyclone performance.

Material chosen for this simulation is dioctyl phthalate (DOP) with density  $980 \text{ kg/m}^3$ . DOP enter the cyclone with air, some of it collected at bottom trap while others escaped at top of the cyclone. Table 1 and Figure 1 show the configuration of Kim and Lee (1990) cyclone. The grid used in this study was generated by pre-processor software, GAMBIT 2.4, contains contains approximately 36000 cells. The grid was made of a high quality pure hexahedral mesh to minimize the turbulent diffusion during the simulation.

Boundary conditions specify the flow and thermal variables on the boundaries of physical model. They are, therefore, a critical component of FLUENT simulations and it is important that they are specified appropriately. The boundary types that were set for this experiment are as follow:

- Inlet set as velocity inlet
- Outlet top set as particle escaped
- Outlet bottom set as particle trap

- Cyclone wall set as standard wall function

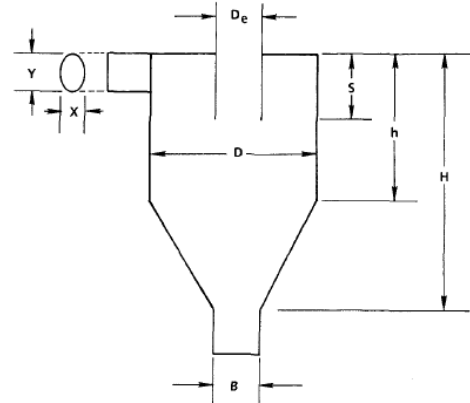


Figure 1: Configuration for cyclone I & II

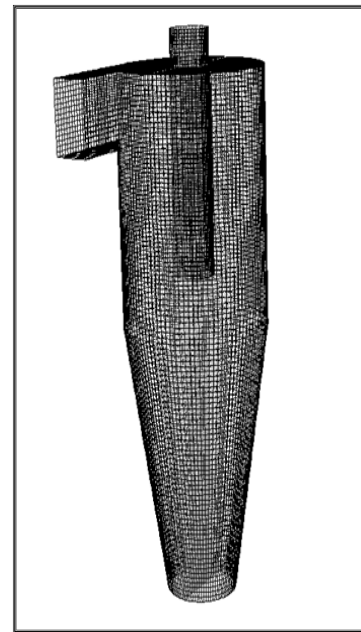


Figure 2: Coarse grid cyclone mesh

| Cyclone | Dimensions (cm)      |                           |      |      |     |     |     |     |
|---------|----------------------|---------------------------|------|------|-----|-----|-----|-----|
|         | Body Diameter, $D_B$ | Exit Tube Diameter, $D_E$ | X    | Y    | S   | h   | H   | B   |
| I       | 3.11                 | 0.8                       | 0.71 | 1.29 | 3.6 | 4.5 | 9.5 | 1.5 |
| II      | 3.11                 | 1.36                      | 0.71 | 1.29 | 3.6 | 4.5 | 9.5 | 1.5 |

Table 1: Dimension of cyclones I & II based on Kim & Lee (1990).

## 2.4 Details on CFD Setting

The details on CFD setting is shown in table 2.

| Details                                     | Setting  |
|---|--|
| <b>Boundary Condition</b>                   |  |
| Inlet                                       | Velocity   |
| Outlet Top                                  | Outflow (particle escape)                                    |
| Outlet Bottom                               | Outflow (particle trap)                                      |
| Cyclone Wall                                | Standard wall function                                       |
| <b>Viscous</b>                              |  |
| Turbulence                                  | Reynold Stress Model (RSM)<br>Detached Eddy Simulation (DES) |
| <b>Discretization</b>                       |  |
| Pressure                                    | Presto!  |
| Pressure-velocity Coupling                  | 2 <sup>nd</sup> Order Upwind                                 |
| Momentum                                    | 2 <sup>nd</sup> Order Upwind                                 |
| Turbulence Kinetic Energy                   | 2 <sup>nd</sup> Order Upwind                                 |
| Reynold Stresses                            | 2 <sup>nd</sup> Order Upwind                                 |
| <b>Discrete Phase Modelling (DPM)</b>       |  |
| Assumption                                  | Sphere Particle  |
| Maximum number of Steps (phase integration) | 10000  |

Table 2: Details on CFD setting.

## 3.0 RESULTS AND DISCUSSIONS

The objectives of this study are to understand the influence of inlet velocity and exit tube dimension to miniature aerocyclone performance (collection efficiency, pressure drop) from data predicted by CFD simulation. At the same time, performance of two different turbulence model implemented in CFD can be analyzed, from view of prediction accuracy. Both turbulent models prediction accuracy can be determined by comparing simulation data with experimental data made by Kim & Lee (1990). This section will present the result obtain from simulation in the function of cyclone collection efficiency and pressure drop and result justification.

### 3.1 Cyclone Collection Efficiency

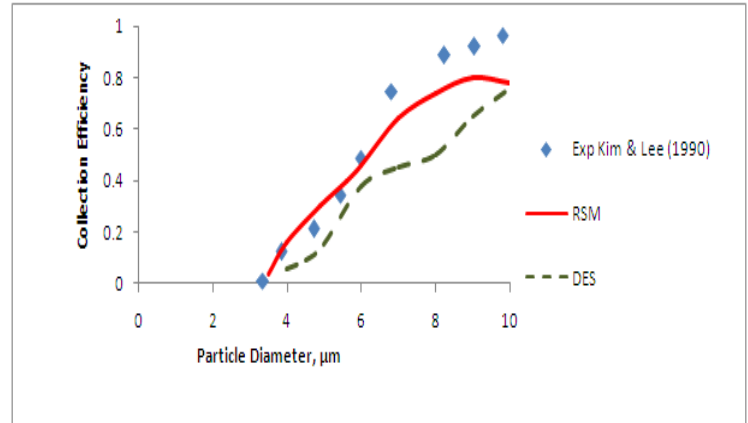
Cyclone collection efficiency is a great indicator of cyclone performance. These mini cyclones are operated under ambient temperature where temperature change is neglected. Many applications of cyclone are operated at normal temperature such saw dust and grain dust removal from air. Kim & Lee (1990) presented their experimental data under room temperature, so the

simulation is set at room temperature. There are two set of cyclone collection efficiency data presented, where both set differ only in exit tube dimension. Cyclone II has larger exit tube diameter than cyclone I, so the exit tube dimension influence on cyclone collection efficiency can be observed. The collection efficiency versus particle diameter is plotted for 3 different inlet velocities, which are 8.8, 12.4 and 18.4 litre/min. Figure 3 shows the comparison between Kim & Lee (1990) experimental data and CFD prediction for Cyclone I ( $D_e = 0.8$  cm) for 3 velocity inlet. Most of the measurement data are seen to projected a so-called “S”- shape curve, with little scatter. Early observation that can be made is the collection efficiency is seen to increase as either the particle size or flow rate increases. Figure 4 shows the comparison between Kim & Lee (1990) experimental data and CFD prediction for Cyclone II ( $D_e = 1.36$  cm) also for 3 different inlet velocity.

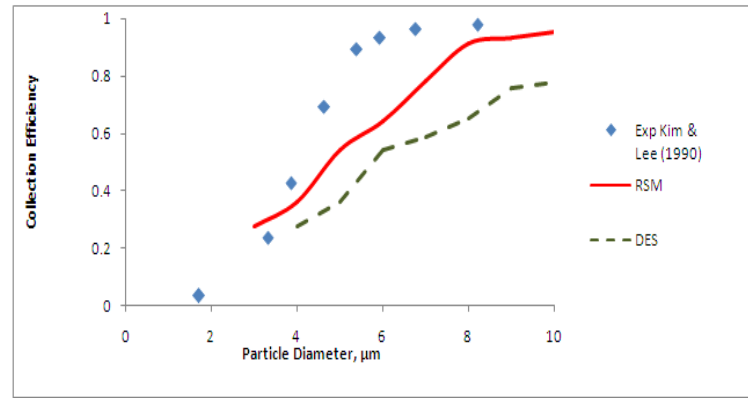
Basically, the two cyclones show the same trend of collection efficiency. Both cyclones demonstrate that collection efficiency increase if either inlet velocity or particle size increase. Increasing inlet velocity increases the centrifugal force and therefore efficiency, but at the same time decreases the pressure drops. From Air Pollution Control Technology Handbook by Schnelle & Brown (2002), increasing gas flow rate through given cyclone will have effect on collection efficiency such as:

$$\frac{Pt_2}{Pt_1} = \left(\frac{Q_1}{Q_2}\right)^{0.5}$$

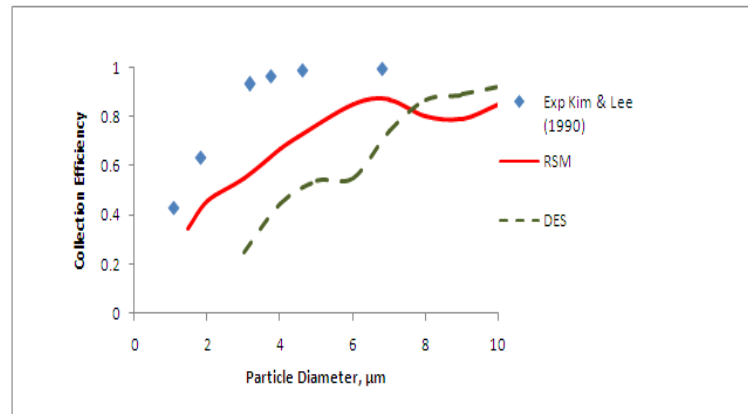
where  $Pt$  is penetration and  $Q$  is volumetric flow rate. Particle penetration is equal to  $1 - \eta$  (particle removal efficiency) and inlet velocity can be determined by dividing volumetric flow with inlet vane area (a.b). The efficiency curve becomes sharper as inlet flow rate increases. Collection efficiency curve is seem sharper as the air flow rates increases, as shown on figure 3 & 4. Shape of collection efficiency curves for a fixed flow rate is seem to remain roughly the same regardless of cyclone body size and exit tube size.



(a)

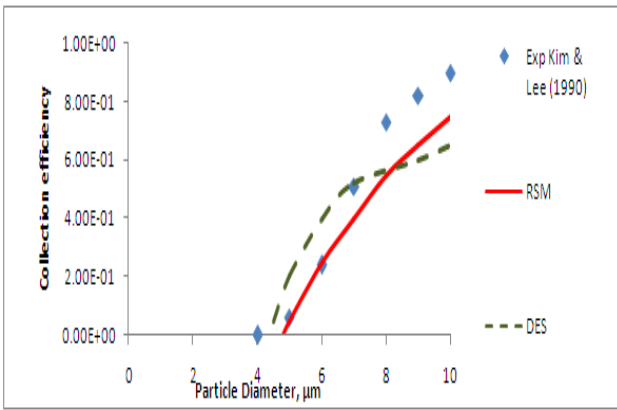


(b)

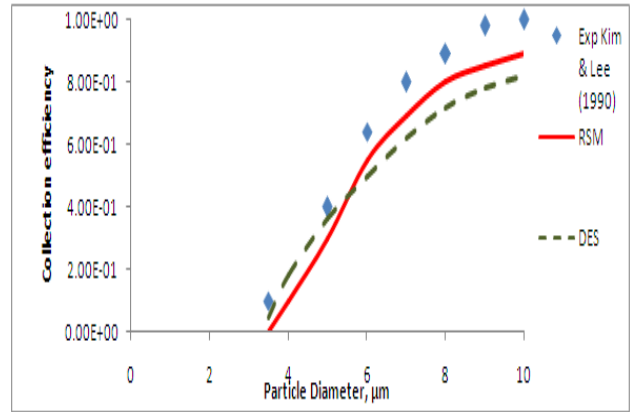


(c)

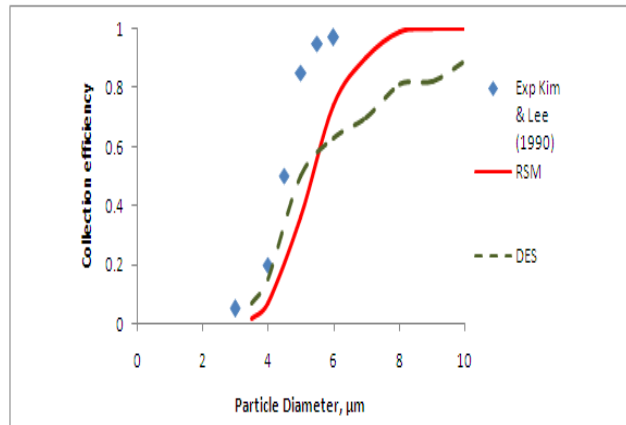
Figure 3: Simulated collection efficiencies for Kim & Lee cyclone I ( $P = 1$  atm,  $T = 273$  K,  $D_e = 0.8$  cm) for different inlet velocities, (a) for 8.8 lpm, (b) for 12.4 lpm and (c) for 18.4 lpm. .



(a)



(b)



(c)

Figure 4: Simulated collection efficiencies for Kim & Lee cyclone I ( $P = 1 \text{ atm}$ ,  $T = 273 \text{ K}$ ,  $D_e = 1.36 \text{ cm}$ ) for different inlet velocities, (a) for 8.8 lpm, (b) for 12.4 lpm and (c) for 18.4 lpm..

Separation of solids from the gas is due to classification in the vortex due to centrifugal forces. The centrifugal force field established by swirling flow inside the entire cyclone. When centrifugal force acts on a particle, it causes a radial settling velocity. This settling velocity is superimposed by an axial flow component. It is obvious that very coarse particle with

high settling velocity will reach the wall and finer particles with a high settling velocity will reach the wall and finer particles may drag to inner vortex where they are classify according to cut size and efficiency grade curve. Main volumetric flow rate and the clarification area will determine whether a particle is separated at the wall or not.

From exit tube size prospect, it is observed that particle collection efficiency is found to decrease with increasing exit tube size. This observation can be seen in figure 5 ( $v_i = 18.4$  lpm) where the larger  $D_e/D$  has lower collection efficiency. For most cyclone design application the ratio of the exit tube to cyclone body is kept roughly the same, so the change in particle size with quite big magnitude is not widely recognized. The influence of exit tube size toward collection efficiency is seen significant as it manipulate both inner and outer spiral flow pattern. If diameter of the exit tube is large, the flow pattern may not be sharp, so the particle may likely exit at the top outlet without reaching the bottom part of the cyclone. Small exit tube size will induce a well defined outer spiral flow and small and long inner spiral flow forcing larger number of particle to travel via bottom part of the cyclone, thus increasing the chances of the particles to fall into bottom trap.

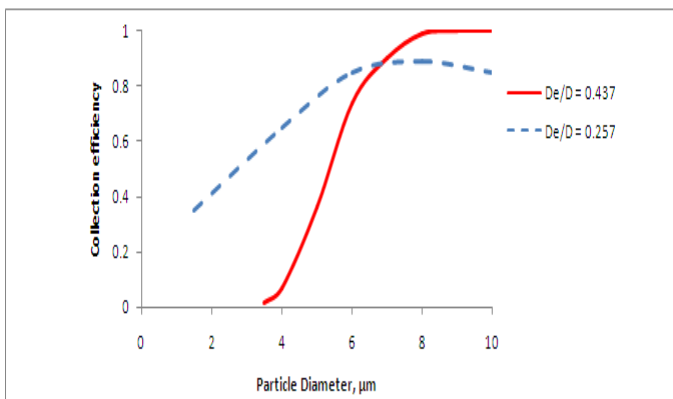


Figure 5: Simulated collection efficiencies for Kim & Lee cyclone II ( $P = 1$  atm,  $T = 273$  K,  $v_i = 18.4$  lpm,  $D_e = 1.36$  cm). Data point from Kim and Lee (1990).

Both turbulence model predict the expected s-curve of cyclone collection efficiency, where RSM shown excellent agreement with Kim & Lee (1990) experimental data. Fraser (2003) describe that Reynolds Stress turbulence model yields an accurate prediction of swirl flow pattern, axial velocity, tangential velocity and pressure drop on cyclone simulations. The thoroughness of this model numerically solving as much as 7 equations, the

performance is as expected. Besides, RSM has been favorite numerical approach among researchers since its introduction. Meanwhile, DES prediction did follow the 's' shape curve but not as precise and collection efficiency seldom reach 1 as it supposed when reaching particular particle diameter. DES inability is due to its incompatibility simulating the multiphase separation occurred inside the cyclone

Separation of particles in the cyclone is due to the centrifugal force caused by the spinning gas stream; this force throws particles outward to the cyclone wall. Opposing this outward particle motion is an inward drag force caused by gas flowing toward the axis of the cyclone prior to discharge. The centrifugal force developed inside the cyclone accelerates the settling rate of the particles, thereby separating them according to specific gravity in the medium. Denser particle is flung to the outer wall of the cyclone where the settling velocity is at its lowest and progresses downwards along the cyclone wall in a spiral flow pattern until it exits at the bottom cone. For smaller particles, the drag force maybe sufficient to move the particle towards the center of the cyclone. If the inward drag force is strong enough, and particles reach the central flow region where the flow is ascending, they will most likely escape together with the outgoing gas. However, the centrifugal force will increase, as the particle is moving towards the radius of the outlet pipe due to the increased tangential velocity. Thus the force on a particle may balance at some radius where the particle theoretically stops its radial movement and revolves in an orbit with constant radius. Shephred et al. (1939) wrote that particle can also change path due to secondary effects such as turbulence eddies or collision with other particles. At the bottom cone, a reverse vortex begins to form creating a low pressure zone flowing upwards along the axis of the cyclone, through vortex finder and exit at the overflow.



### 3.2 Cyclone Pressure Drop

Pressure drop across the cyclone is a great indicator of cyclone power usage. Pressure drops provide driving force that generates gas velocity and centrifugal force inside the cyclone. An accurate prediction of pressure drop will directly determine operating cost of a cyclone. In this study pressure drop of a cyclone is calculate as pressure difference between inlet pressure and top outlet pressure. Basically, many researchers found that cyclone pressure drop is directly proportional to inlet velocity. The Air Pollution Control Technology Handbook by Schnelle & Brown ( 2002) gives the correlation between pressure drop and inlet velocity of the cyclone as:

$$\Delta P = \frac{1}{2g_c} \rho_g V_i^2 N_H$$

where  $\Delta P$  = pressure drop

$\rho_g$  = gas density

$V_i$  = inlet gas velocity

$N_H$  = pressure drop expressed as number of the inlet velocity heads

The simulations of both RSM and DES models show the same agreement. Pressure drop of both cyclone I & II are both compared with Kim & Lee (1990) for two different inlet velocities as shown in table 3. It should be noted RSM prediction of both model shows excellent agreement with experimental data for both cyclones while DES prediction shown fair agreement with experimental with error less than 30%. This is due to incompatibilities of DES model in

predicting multiphase (air & particle) condition of the cyclone.

The pressure drop was found to decrease with increase on exit tube diameter. If exit tube size is enlarged until it reaches the diameter of cyclone body, the pressure drop will increase again. Kim and Lee (1990), describe that the reduces in pressure drop when the exit diameter become larger happens due to significant portion of pressure drops occur inside the exit tube. When the exit tube diameter too large, the sudden increase of pressure drop indicates that energy loss occurs in the annular gap between exit tube and cyclone wall.

Generally, two factors that induce pressure drops across the cyclone are the wall friction and the contraction of the inner vortex on entering the vortex finder. Two parts in the cyclone contribute the total pressure drops across the cyclone. The first part is pressure lost in the separation zone, caused by the friction between gas and solid surface. Separation zone pressure loss contributes about 80% of total pressure drop, depending on tangential velocity, the radius and the mean axial velocity, the surface area, and wall friction. Another 20% of pressure drops is contributed by pressure loss occurs in vortex finder or exit tube section, which being manipulated in this study. The pressure loss of vortex finder can be determined by relationship between tangential velocity, the radius and the mean axial velocity in exit tube of a cyclone.

| Cyclone-I Pressure Drop (Pa)  |           |           |              |
|-------------------------------|-----------|-----------|--------------|
| Inlet Velocities              | RSM Model | DES Model | Experimental |
| 12.4                          | 31.236    | 37.65     | 27.4         |
| 18.4                          | 69.32     | 72.33     | 60.279       |
| Cyclone-II Pressure Drop (Pa) |           |           |              |
| Inlet Velocities              | RSM Model | DES Model | Experimental |
| 12.4                          | 16.44     | 21.4      | 13.7         |
| 18.4                          | 52.7      | 49.8      | 43.59        |

Table 3: Fluent predictions for cyclone I & II pressure drop. Experimental data obtained from Kim and Lee (1990).

### 3.3 Particle 50% Cut-Off Size

Several methods for estimating cyclone efficiency have been developed. Most of these methods utilize a particle size term called a 50 % particle cut size. 50 % particle cut size can be defined as particle diameter taken when collection efficiency equals to 50%. The  $d_{50}$  cut size corresponds to a size where 50% of particles smaller than  $d_{50}$  and 50% of particles larger than  $d_{50}$  will be collected. 50 % particle cut size is usually utilized in order to compare an increased number of the data sets with theories in systematic ways. As in this study, the effect of exit tube diameter can be studied using  $d_{50}$ . Table 4 shows the comparison between 50% cut-off diameter between CFD prediction and experimental data by Kim & Lee (1990).

Both model RSM and DES prediction shows excellent agreement with experimental data, even though DES still lacking in precision compared to RSM due to its incompatibilities. The cut 50% cut off diameter decreases when velocity increases, and at the same time demonstrate that  $d_{50}$  increases with increases exit diameter. The latter observation supports that efficiency curve become stiffer with increasing inlet velocity. Somehow, if the flow rate is fixed, efficiency curve cease to change even with change in exit diameter. So it is possible to alter the diameter particle without deteriorating sharpness just by simply adjusting the exit tube diameter.

| <b>Cyclone-I 50% Cut-Off Diameter</b>  |                  |                  |                     |
|--|------------------|------------------|---------------------|
| <b>Inlet Velocities</b>                | <b>RSM Model</b> | <b>DES Model</b> | <b>Experimental</b> |
| 8.8                                    | 5.97             | 6.5              | 6.1                 |
| 12.4                                   | 4.5              | 5.4              | 4.2                 |
| 18.4                                   | 2.4              | 4.0              | 1.806               |
| <b>Cyclone-II 50% Cut-Off Diameter</b> |                  |                  |                     |
| <b>Inlet Velocities</b>                | <b>RSM Model</b> | <b>DES Model</b> | <b>Experimental</b> |
| 8.8                                    | 6.8              | 5.9              | 6.6                 |
| 12.4                                   | 5.3              | 5.3              | 5                   |
| 18.4                                   | 5                | 4.8              | 4.5                 |

Table 4: Fluent predictions for cyclone 50% cut-off diameter. Experimental data obtained from Kim and Lee (1990)

### 4.0 CONCLUSIONS

The CFD code predicts very well the collection efficiency, pressure drop and cut-off size of Kim & Lee experimental miniature cyclone. Two turbulence models were used in this study, the RSM and DES. The RSM model was found to be much closer to experimental data compared to DES model. DES liability was due to its incompatibilities in simulating multiphase condition of cyclone separation, in this case between gas (air) and solids (DOP particles). Simulation data revealed that increases inlet velocity will make efficiency curve stiffer, or the  $d_{50}$  become

smaller. With respect to exit tube size, particle collection efficiency is found to increase when exit tube size become smaller. It is believed that the exit tube size largely influencing the flow field inside the cyclone, including the pattern of the outer and the inner spiral flows. Pressure drops simulation shown that the pressure drop across the cyclone to be dependent on cyclone flowrate. As exit tube increases, the pressure drop was found to be decreased. Also, when exit tube size increased until as large as cyclone body, the pressure drops increase again. Cut-off diameter was simulated to clearly shows the relationship between  $d_{50}$  and the cyclone exit tube size diameter which directly proportional.

## Notation

|                 |  |
|-----------------|--|
| a               | Cyclone inlet height (m)                 |
| b               | Cyclone inlet width (m)                  |
| D               | Cyclone body diameter (m)                |
| D <sub>e</sub>  | Cyclone gas outlet diameter (m)          |
| H               | Cyclone height (m)                       |
| h               | Cyclone cylinder height (m)              |
| S               | Cyclone gas outlet duct length (m)       |
| B               | Cyclone dust outlet diameter (m)         |
| $\rho_g$        | Gas density (kg/m <sup>3</sup> )         |
| u, v            | Inlet velocity (m/s)                     |
| Re <sub>r</sub> | Relative Reynolds number                 |
| C <sub>D</sub>  | Drag coefficient                         |
| $\tau_v$        | Particle response time                   |
| $\rho_p$        | Particle density (kg/m <sup>3</sup> )    |
| $\mu_g$         | Gas viscosity (m <sup>2</sup> /s)        |
| d <sub>p</sub>  | Particle diameter (m)                    |
| r               | Radius (m)                               |
| v <sub>c</sub>  | Tangential velocity along the path (m/s) |
| $\omega$        | Angular velocity (rad/s)                 |
| m               | Mass (kg)                                |
| F <sub>c</sub>  | Centrifugal force (kg m/s <sup>2</sup> ) |
| F <sub>g</sub>  | Gravity force (kg m/s <sup>2</sup> )     |

## References

- D. Leith, W. Licht, The collection efficiency of cyclone type particle collectors: a new theoretical approach, *AIChE Symposium Series* 68 (1972) 196–206.
- J. Gimbut, T.G. Chuah, A. Fakhru'l-Razi, Thomas S.Y. Choong, The influence of temperature and inlet velocity on cyclone pressure drop: a CFD study, *Chemical Engineering and Processing* 44 (1) (2005) 7 – 12.
- Kim, J. C. and Lee, K. W. (1990) Experimental Study of Particle Collection by Small Cyclones. *Aerosol Sci. Technol.* 12, 100331015.
- T.G. Chuah, J. Gimbut, Thomas S.Y. Choong, A CFD study of the effect of cone dimensions on sampling aerocyclones performance and hydrodynamics, *Powder Technology* 162 (2006) 126 – 132.
- Moore, M. E., & McFarland, A. R. (1990). Design of Stairmand-type sampling cyclones. *American Industrial Hygiene Association*, 51, 151–159.
- T. Fraser, Personal Communication, fraser1@cf.ac.uk, www.cfd-online.com, 2003.
- Saltzman, B. (1984) Generalised performance characteristics of miniature cyclones for atmospheric particulate sampling. *Am. Ind. Hyg. Assoc. J.* 45, 671-680.
- Iozia, D. L. and Leith, D. (1989) Effect of cyclone dimensions on gas flow pattern and collection efficiency. *Aerosol Sci. Technol.* 10, 491-500.
- Lapple, C. E. (1950) Gravity and centrifugal separation. *Znd. Hyg. Q.* 11, 40
- W. Barth, Berechnung und Auslegung von Zyklonabscheidern aufgrund neuerer Untersuchungen, *Brennstoff, Wärme, Kraft* 8 (1956) 1– 9.
- Chen, C. C., Lai, C. Y., Shih, T. S., & Yeh, W. Y. (1998). Development of respirable aerosol samplers using porous foams. *American Industrial Hygiene Association*, 59, 766–773.
- Petty, C.A., Parks, S.M., Shao, S.M., 2000. The use of small hydrocyclones for downhole separation of oil and water. Svarovsky, L., Thew, M. (Eds.), 5th International Conference on Cyclone Technologies. BHR Group Limited, The Fluid Engineering Centre, Cranfield, Bedfordshire
- Tsai, C. J., Chein, H. M., Chang, S. T., & Kuo, J. Y. (1996). Performance evaluation of an API aerosizer. '96 International Conference on Aerosol Science and Technology, Taipei, Taiwan (pp. 559–568).
- Wu, J. J., Copper, D. W., & Miller, R. J. (1989). Virtual impactor aerosol concentrator clean room monitoring. *Journal of the Environmental Science*, 32, 52–56.
- Smith, W. B., Cushing, K. M., & Wilson, R. R. (1982). Cyclone sampling for measuring the concentration of inhalable particles in process streams. *Journal of Aerosol Science*, 13, 259–267.
- Saltzman, B. E., & Hochstrasser, J. M. (1983). Design and performance of miniature cyclone for respirable aerosol sampling. *Environmental Science and Technology*, 17, 418–424.
- Shepherd, G. B. and Lapple, C. E. (1939) Flow pattern and pressure drop in cyclone dust collectors. *Ind. Eng. Chem.* 31, 972.
- W.D. Griffiths, F. Boysan, Computational fluid dynamics (CFD) and empirical modelling of the performance of a number of cyclone samplers, *Journal of Aerosol Science* 27 (1996) 281–304.
- Zhu, Y., & Lee, K. W. (2001). Experimental study on small cyclones operating at high flow rates. *Journal of Aerosol Science*, 30, 1303–1325.